UHASSELT
KNOWLEDGE IN ACTION

Maastricht University

Faculteit Geneeskunde en Levenswetenschappen
School voor Levenswetenschappen

master in de biomedische wetenschappen

Masterthesis

The neuroregenerative aspects of insulin-like growth factor-2 enhanced dental pulp stem cells as a therapy for ischemic stroke

Olivier Rodiers

Scriptie ingediend tot het behalen van de graad van master in de biomedische wetenschappen, afstudeerrichting klinische moleculaire wetenschappen

PROMOTOR :
Prof. dr. Annelies BRONCKAERS

COPROMOTOR :
Prof. dr. Esther WOLFS

BEGELEIDER :
De heer Yorg DILLEN

2018
2019

De transnationale Universiteit Limburg is een uniek samenwerkingsverband van twee universiteiten in twee landen: de Universiteit Hasselt en Maastricht University.

UHASSELT
KNOWLEDGE IN ACTION

www.uhasselt.be
Universiteit Hasselt
Campus Hasselt:
Martelarenlaan 42 | 3500 Hasselt
Campus Diepenbeek:
Agoralaan Gebouw D | 3590 Diepenbeek

Faculteit Geneeskunde en Levenswetenschappen

School voor Levenswetenschappen

master in de biomedische wetenschappen

Masterthesis

The neuroregenerative aspects of insulin-like growth factor-2 enhanced dental pulp stem cells as a therapy for ischemic stroke

Olivier Rodiers

Scriptie ingediend tot het behalen van de graad van master in de biomedische wetenschappen, afstudeerrichting klinische moleculaire wetenschappen

PROMOTOR :
Prof. dr. Annelies BRONCKAERS

COPROMOTOR :
Prof. dr. Esther WOLFS

BEGELEIDER :
De heer Yorg DILLEN

Acknowledgements

I was always fascinated by the endless possibilities of stem cells and tissue regeneration. Repairing damage in the brain with the use of stem cells sounded like the holy grail of science to me. This interest lead me to perform my senior internship within the group of morphology. Here I learned my first tricks of the trade of being a scientist and discovered my passion for fluorescence microscopy. I noticed that performing science does not only involve, precision, criticism, and knowledge, but that a lot of perseverance and optimism are required to become a great scientist. Taking hindrances and accomplishing something in science is a team effort. Therefore, I would like to thank some of the people who helped and supported me this year.

First of all, I would like to thank Prof. dr. Annelies Bronckaers my promotor. Her trust and believe in me gave me the confidence to make decisions, plan experiments and undertake my lab work as an independent scientist. Her enthusiasm for science is inexhaustible. This inspired me and will inspire many more to come.

Also, many thanks go to my daily supervisor Yörg Dillen. His criticism for good science, eye for detail, and impressive knowledge about neurogenesis encouraged me to work harder, learn more and improve myself. He is a scientist to look up to. (May the force be with you! ;))

Next, I would like to thank Prof. dr. Esther Wolfs, my co-promotor for her advice during the lab meetings. Also, I like to thank her and Leen Rasking for all the help with cloning. Their persistence to generate the correct lentiviral vector will be rewarded (I believe in it!). Further, I would thank my second examiner Prof. dr. Virginie Bito for her advice during this project.

A word of appreciation goes out to dr. Pascal Gervois, dr. Tim Vangansewinkel, dr. Ronald Driesen, Greet Merckx, Hannelore Kemps, and Melissa lo Monaco of the group of morphology. Whether I had questions or problems, they were always there to help me. Further, I would also like to thank Jeanine Santermans to help me with the immunostainings.

Special thanks go to all my senior colleagues, for all the laughter’s, fun times and coffee breaks. It was a pleasure sharing an office with you all. At last, I would like to thank my family, friends, and my girlfriend Kaat, for the support, the motivational words and the believe in me.

Table of contents

Abbreviations

2,3,5-Triphenyl-tetrazolium chloride **(TTC)**

4',6-Diamidino-2-phenylindole **(DAPI)**

Adenosine triphosphate **(ATP)**

Base pairs **(BP)**

Blood flow **(BF)**

Blood-brain barrier **(BBB)**

Bone marrow-derived mesenchymal stem cells **(BM-MSC)**

Brain derived neurotrophic factor **(BDNF)**

Conditioned medium **(CM)**

Diaminobenzidine **(DAB)**

Dimethyl sulfoxide **(DMSO)**

Distal middle cerebral artery occlusion **(dMCAO)**

Doublecortin **(DCX)**

Enzyme linked immunosorbent assay **(ELISA)**

Epidermal growth factor **(EGF)**

Ethylenediaminetetraacetic acid **(EDTA)**

Fetal bovine serum **(FBS)**

Fibroblast growth factor 2 **(FGF-2)**

Glial fibrillary acidic protein **(GFAP)**

Green fluorescent protein **(GFP)**

Horse radish peroxidase **(HRP)**

Human dental pulp stem cells **(DPSC)**

Human dermal fibroblasts **(HDF)**

Human microvascular endothelial cells **(HMEC-1)**

Insulin-like growth factor **(IGF)**

Insulin-like growth factor binding protein **(IGFBP)**

Interleukin **(IL)**

Intra-cerebroventricular **(ICV)**

Ionized calcium-binding adapter molecule-1 **(IBA-1)**

Mesenchymal stem cells **(MSC)**

Neural progenitor cellS **(NPC)**

Neural stem cell **(NSC)**

Neuronal Nuclei **(NeuN)**

Paraformaldehyde **(PFA)**

Perilesional **(PL)**

Phosphate buffered saline **(PBS)**

Polysialylated-neural cell adhesion molecule **(PSA-NCAM)**

Reactive oxygen species **(ROS)**

Recombinant tissue plasminogen activator **(r-tPA)**

SRY (sex determining region Y)-box 2 **(SOX2)**

Standard error of the mean**(SEM)**

Stromal derived factor 1 **(SDF-1)**

Subventricular zone **(SVZ)**

Tumor necrosis factor alpha **(TNF-α)**

Vascular endothelial growth factor **(VEGF)**

Abstract

Background: Stroke is a major cause of disability and is the second leading cause of death worldwide. Current therapies are only applicable to a minority of the patients, highlighting the need for new treatments. A stroke can be defined as a sudden alteration in the cerebral blood flow, resulting in a loss of brain function. A promising alternative therapeutic approach is the use of human dental pulp stem cells (DPSC), which is devoted to their secretory character. During this study, the IGF-2 expression levels of insulin-like growth factor 2 (IGF-2) by DPSC were first investigated. Next, it was examined whether IGF-2 and two engineered IGF-2 variants Des[1-6], and Arg6 improve neurogenesis and angiogenesis *in vitro*. The final goal is to use the most potent variant in a DPSC cell-line to enhance the neuroregenerative effects of DPSC.

Materials and methods: Firstly, the IGF-2 expression levels of DPSC were examined by an ELISA. Next, the effects of IGF-2 and the IGF-2 variants Des[1-6] and Arg6 on the migration of neural stem cells (NSC) and human microvascular endothelial cells (HMEC) were examined employing a transwell migration assay. Furthermore, a lentiviral DNA construct containing the most potent IGF-2 variant was generated for transduction into the DPSC. Additionally, two modes of DPSC transplantation were compared in a mouse model of stroke (distal middle cerebral artery occlusion mouse model (dMCAO)).

Results: DPSC produce more IGF-2 than bone marrow-mesenchymal stem cells (BM-MSC) and then human dermal fibroblasts (HDF). As a result, DPSC were chosen as an ideal stem cell to generate an IGF-2-enhanced cell line. Next, it was seen that IGF-2 and its variants stimulate the migration of NSC. Furthermore, these IGF-2 variants show to be less sensitive to inhibition by IGFBP-6, an endogenous inhibitory binding protein of IGF-2. IGF-2 and the IGF-2 analogs were also able to induce HMEC-1 migration. Consequently, the Des[1-6] variant was implemented in a lentiviral DNA construct which will be used for transduction of DPSC. Furthermore, stereotactic transplantation of DPSC both in the perilesional area and the intraventricular space were successful and survival of the DPSC for at least seven days was observed after perilesional transplantation.

Conclusion: IGF-2 and the IGF-2 variants can enhance NSC and HMEC-1 migration *in vitro,* and the IGF-2 variants were revealed to be less prone for IGFBP-6 inhibition when inducing NSC migration. Based on these results, the Des[1-6] IGF-2 analog was chosen as the most potent variant. It shows to have great promise for therapeutic interventions by transplantation of IGF-2-enhanced DPSC after stroke. Further research in rodent stroke models is required to validate the beneficial effects of Des[1-6] IGF-2-enhanced DPSCs.

Samenvatting

Achtergrond: Een herseninfarct is wereldwijd de meest voorkomende doodsoorzaak, deze ziekte leidt tevens ook frequent tot fysieke beperkingen. Huidige behandelingen zijn enkel van toepassing voor een kleine groep van patiënten. Er is tevens een gebrek aan nieuwe therapieën. Een herseninfarct kan gedefinieerd worden als een plotse verstoorde bloedtoevoer naar de hersenen. Dit kan leiden tot een verlies van hersencapaciteit. Een veelbelovende alternatieve therapie is het gebruik van humane dentale pulpa stamcellen (DPSC). Deze beschikken over een hoge secretie van paracriene factoren. Tijdens deze studie werd het "insulin-like growth factor-2" (IGF-2) expressie gehalte van de DPSC in kaart gebracht en werd er gekeken of deze stamcellen succesvol konden worden getransplanteerd in muizen met een beroerte. Vervolgens, werd onderzocht of IGF-2 en twee IGF-2 varianten Des[1-6] en Arg6 neurogenese en angiogenese *in vitro* konden induceren. Als einddoel werd de meest optimale IGF-2 variant gebruikt voor het maken van een IGF-2-DPSC-cellijn.

Materiaal en methoden: Eerst werd het IGF-2 expressie gehalte van de DPSC onderzocht met behulp van een ELISA. Vervolgens werden de effecten van IGF-2 en de IGF-2 varianten Des[1-6] en Arg6 op de migratie van neurale stamcellen (NSC) en humane microvasculaire endotheelcellen (HMEC-1) onderzocht. Ook werd er een lentiviraal DNA construct met IGF-2 gemaakt dat nodig was voor het genereren van een IGF-2-DPSC-cellijn. In toevoeging, werden twee injectiemethodes voor de transplantatie van DPSC in een muismodel getest.

Resultaten: DPSC produceerde meer IGF-2 dan mesenchymale stamcellen uit het beenmerg (BM-MSC) en dan humane dermale fibroblasten (HDF). De DPSC werden hierdoor gekozen als ideale stamcel voor het maken van een IGF-2 stamcellijn. Vervolgens, zijn IGF-2 en de IGF-2 varianten in staat om NSC migratie te stimuleren. In toevoeging, blijken deze varianten minder gevoelig te zijn voor inhibitie van "insulin-like growth factor-binding protein-6" (IGFBP-6). Ook zijn deze varianten in staat om net als IGF-2, migratie van HMEC-1 te induceren. Als gevolg werd de Des[1-6] IGF-2 variant gebruikt voor het maken van een lentiviraal DNA construct, nodig voor het transduceren van de DPSC. Na DPSC transplantaties blijkt de perilesionale transplantatiemethode de meest succesvolle, waarbij de DPSC voor minsten zeven dagen kunnen overleven.

Conclusie: IGF-2 en de IGF-2 varianten kunnen *in vitro* NSC en HMEC-1 migratie induceren, waarbij de IGF-2 varianten minder gevoelig zijn voor IGFBP-6 inhibitie tijdens het genereren van NSC migratie. De Des[1-6] IGF-2 variant werd gekozen als meest optimale IGF-2 variant. Op basis van deze resultaten kan geconcludeerd worden dat deze variant veel potentieel heeft om gebruikt te worden tijdens therapeutische interventies na een herseninfarct, waarbij een IGF-2 cellijn wordt gebruikt. Verder onderzoek in diermodellen is noodzakelijk om de effecten van deze Des[1-6] IGF-2-DPSC aan te tonen.

1. Introduction

Annually, stroke is responsible for 10-15% of the worldwide mortality, making it the world's second leading cause of death (1). Moreover, stroke is the third most common cause of disability (2). Survivors of a stroke suffer from severe health consequences and limitations; often, these patients have a shortened life span and an increased risk of a recurrent stroke (3). A stroke is defined as a sudden cerebral dysfunction evoked by a decline in the blood supply to the brain. This condition can be divided into two main subtypes. Ischemic stroke, induced by a vascular occlusion, is the most common type and accounts for 80-85% of the worldwide stroke prevalence. The second one, hemorrhagic stroke, is caused by intracerebral bleeding (20-25%) (4, 5).

The vascular occlusion during ischemic stroke is induced by an embolism or thrombus, which can originate from atherosclerosis, small vessel diseases, cardiac pathologies, dissection, or other causes (6, 7). The alteration in cerebral blood flow results in an oxygen and glucose deprived area, which initiates a cascade of processes leading to neural cell death. Depending on the affected brain area, the outcome of a stroke is variable. Hence, the consequences of this condition are very versatile, altering from neurological and functional impairments to social and psychological problems (8).

1.1. Pathophysiology of ischemic stroke

The reduction in cerebral blood flow during ischemic stroke results in an ischemic lesion and can be subdivided into three areas based on the level of perfusion. Within the core of the lesion, the blood flow (BF) is reduced to approximately 80%. This event leads to the depolarization of the cell membranes and results in irreversible tissue loss. The ischemic core is surrounded by the penumbra, an area with a BF reduction of 50-75%. If the BF is not restored within hours or days, cell death will occur. The penumbra is enclosed by a slightly hypo-perfused area defined as benign oligemia, in which the cells will survive (9, 10).

Due to the oxygen and glucose deprivation, the cells within the lesion have to switch to their anaerobic energy metabolism. The anaerobic degradation of one glucose molecule results in an energy output of two adenosine triphosphate (ATP) molecules. This anaerobic process is, in contrary to the 38 ATP molecules produced during the aerobic degradation, not sufficient to replete the required energy needs. As a consequence, the cells will experience an ATP depletion (11). The shortage of energy halts the ion pumps, leading to an intracellular Ca^{2+}, Na^{+}, and H^{+} accumulation and an elevated extracellular K^{+} efflux (12). The ion misbalance depolarizes the cells and triggers the release of glutamate in the extracellular environment. Consequently, the extracellular glutamate induces a depolarization wave which will affect and damage the adjacent cells contributing to the expansion of the lesion (13). As a consequence, the lack of ATP and accumulation of ions will induce cellular swelling. Eventually, the Ca^{2+} build-up results in the production of reactive oxygen species and the activation of intracellular enzymatic cascades (12). Accordingly, this will lead to mitochondrial and cell membrane damage, with cell death by necrosis

or apoptosis as a final endpoint. Besides the previously mentioned events, secondary damage also occurs post-stroke and is caused by inflammation, oxidative stress, and increased blood-brain barrier (BBB) permeability. These events will contribute to additional cell death and lesion expansion (11, 14, 15). Paradoxically, reperfusion does not necessarily lead to a better recovery. The restoration of the blood flow can cause an ischemia-reperfusion injury, which is characterized by an increase in oxidative stress, more leukocyte infiltration, mitochondrial damage, platelet activation and aggregation, BBB disruption, and complement activation. Because the time of recanalization is proportionally correlated with the adverse effects caused by reperfusion, fast restoration of the blood flow is required to limit the impact of the reperfusion injury (16, 17).

1.2 Current treatments for ischemic stroke

The current treatments for stroke are limited to a few successful procedures. The standard therapies for ischemic stroke focus on an early recanalization. Currently, the most commonly applied intervention is intravenously administered 'recombinant tissue plasminogen activator' (r-tPA), also known as thrombolysis. r-tPA is a thrombolytic agent and causes fibrin-based blood clots to dissolve by cleaving plasminogen to plasmin (18). When administered within a timeframe of 4.5-6 hours, r-tPA is shown to improve the neurological outcome at 3 to 6 months post-stroke. Intravenous thrombolysis cannot be applied to patients with internal bleedings or coagulation problems, which are contraindications often seen in stroke patients. As a result of the small timeframe for successful intervention, and the risks regarding a hemorrhage, r-tPA can only be administered to a limited population (19).

Another treatment strategy which gained popularity the last decennium is the surgical removal of the blood clot with a catheter, better known as mechanical thrombectomy. First generation devices remained unsuccessful, but after improvements, mechanical thrombectomy showed to be potent for the treatment of ischemic stroke (20, 21). Current devices exist of a retrievable stent combined with a mesh or a thrombo-aspirating element to remove the blood cloth (22). Nowadays, both intravenous thrombolysis and mechanical thrombectomy are often combined in the clinic. When applied together, intravenous thrombolysis is used to reduce the blood clot size. Subsequently, thrombectomy is performed to remove the remaining obstruction completely. This is shown to improve successful recanalization rates and reduce mortality (23-25).

A key component of stroke care is physiotherapeutic revalidation. The goal of physiotherapy is to improve the functional abilities of the patient (26). The general rehabilitation strategy is directed towards task-specific training aiming to improve motor control. In addition, it can be combined with strength training to restore muscle mass (27). So far, no clear consensus is reached about the optimal timing to start rehabilitation. It is known that an early intervention commencing 24h post-stroke is beneficial for the patient. However, starting physiotherapy within the first 24h resulted in a more unfortunate outcome (28).

In conclusion, the current treatment procedures are minimal and unable to treat the whole population of stroke patients. Therefore, further research to develop new potent therapies for ischemic stroke remains necessary.

1.3. Potential neuroregenerative treatment strategies

Much ongoing research, as well as the existing therapies (thrombolysis and thrombectomy), possess a neuroprotective approach. The goal of this strategy is to rescue the tissue at risk (i.e., the penumbra) and prevent additional secondary damage. Neuroprotective treatments cannot repair damaged brain tissue. Hence, alternatives are necessary to stimulate the regain of functions that are lost beyond the reach of neuroprotective approaches. This result could be obtained by neuroregenerative therapies aiming to recover tissue damage or to reinforce the surrounding of the lesion. A variety of beneficial methods can be adopted, such as altering the immune system, white matter remodeling, neurovascular remodeling, angiogenesis, and neurogenesis.

1.3.1. Immunomodulation

The stroke-induced immune response contributes to additional neuronal damage after the acute phase of a stroke. The necrotic cells in the ischemic core release signal molecules such as danger-associated molecular patterns, reactive oxygen species (ROS), glutamate, and ATP. Consequently, this results in the activation of microglia, astrocytes, and endothelial cells and thereby mediate the recruitment of macrophages, neutrophils, and lymphocytes by the release of pro-inflammatory molecules. Besides, the blood-brain barrier becomes more permeable as a result of the endothelial activation. This occurrence enables the systemic leukocytes to easily enter the brain 24h post-stroke (29, 30).

The influence of the entry of immune cells on the outcome of a stroke is still controversial. Increasing inflammation acts as a double-edged sword on the pathology of stroke. Depending on the time that went by, the type of stroke, and the lesion site, different immune cells with shifting phenotypes and effects will populate the ischemic brain (31). For example, activated microglia and macrophages secrete a variety of molecules, such as interleukin-1 beta (IL-1β), ROS, and tumor necrosis factor alpha (TNF-α), which are considered to be neurotoxic (32). On the other hand, macrophages were shown to have a neuroprotective effect in murine stroke models by the secretion of transforming growth factor beta (33). The infiltration of T-cells is generally accepted to aggravate the outcome of stroke. This effect is mainly caused by the T-helper-1 cells through the secretion of pro-inflammatory cytokines, such as interleukin-2 (IL-2), IL-12, and interferon-c. However, the presence and secretions of T-helper-2 cells have neuroprotective effects in the ischemic brain (34). Regulatory T-cells are considered to be immunomodulatory cells promoting a positive outcome in stroke. Nonetheless, Treg cell depletion was seen to induce or decrease ischemic brain damage depending on the applied method (35). Although much controverting articles around the effects of B-cells were published, the general idea that B-cells fulfill a neuroprotective role, for example, by the secretion of IL-10, becomes more accepted (35).

Potential therapeutic options could be the use of carefully chosen immunosuppressing or immunomodulatory agents, some of which are shown to have beneficial effects on the outcome of stroke in humans. The use of an IL-1 receptor agonist, for example, indicated to be promising during phase II clinical trials (36, 37). Although the idea of immunomodulation in stroke is hopeful.

The controversies and lack of knowledge about the immune system in stroke complicate the use of such immunotherapies.

1.3.2. White matter remodeling

Not only the gray matter is affected by ischemia. The white matter mainly exists of axons, oligodendrocytes, and astrocytes. It takes up about 40% of the total brain volume. Further, white matter contains less collateral blood vessels then gray matter and is therefore even more sensitive to an ischemic event (38). Oligodendrocytes insulate the axons of neurons by the formation of myelin sheets and are very sensitive to ischemic conditions. As a result, cell death of the oligodendrocytes results in the loss of neural conductance (39). Methods recovering the whiter matter and promoting remyelination of the damaged axons can be adapted. Many studies have shown the possibilities to induce white matter remodeling in stroke. For example, the use of nicotinamide was shown by whang et al. to enhance oligodendrocyte maturation (40). Further, the compound sildenafil was suggested to improve the formation of new oligodendrocytes, a process better known as oligodendrogenesis (41). Another study from Jiang et al. demonstrated that intravenous injection of neural progenitor cells improved white matter reorganization *in vivo* (42). These indications suggest that white matter remodeling can become a useful target for future therapeutic strategies in ischemic stroke, which certainly requires further attention.

1.3.3. Neurovascular remodeling

The neurovasculature is considered an important therapeutic target. The neurovascular unit consists of the microvascular network and the surrounding astrocytes, neurons, and microglia (43). It functions with a tightly coupled and balanced interaction between the neural activity and the cerebral blood flow, which is regulated by the release of chemical mediators such as nitric oxide and lactate. Equal to the neuronal network, the microvasculature of the brain is severely affected by an ischemic event. Within the first minutes and hours changes in the endothelial cell occur; receptor presentation changes and the endothelial astrocyte-matrix starts to degrade, leading to detachment of astrocytes and leakage of the BBB. The accumulation of the ischemia-induced cellular changes result in a strongly uncoupled neurovascular unit (44, 45).

One of the endogenous attempts to rebalance the neurovascular unit after an ischemic event is the activation of angiogenesis to restore the cerebral blood flow. Angiogenesis, which is one of the mechanisms involved in the formation of new blood vessels, is induced by stroke. It can be defined as the formation of new micro-vessels originating from pre-existing blood vessels and is critical to ensure a fast recanalization. The new vessels are formed as a result of the proliferation, migration, sprouting, and branching of endothelial cells (46).

Improving the vascular surrounding by pro-angiogenic treatments can be beneficial to diminish acute cell damage by the formation of new collateral vessels, and as a result, support the formation of new cells e.g., neurons for a neuroregenerative approach (46). Besides, it was seen that a higher vessel density resulted in prolonged survival in stroke patients (45). One of the

possibilities to enhance angiogenesis could be the use of low-frequency electromagnetic waves which are shown to induce angiogenesis in vitro (47), have a positive effect on oxidative stress (48), and are seen to have a protective effect after tissue damage in the brain (49). Administration of growth factors such as vascular endothelial growth factor (VEGF) and platelet-derived growth factor are shown to be pro-angiogenic and able to improve collateralization in cerebral ischemia (50).

Furthermore, the process of angiogenesis is considered to be tightly coupled and coordinated with neurogenesis (51). Neurogenesis can be defined as the proliferation, differentiation and, integration of neural stem cells (NSC) into adult and functioning neurons (52, 53). Angiogenesis seems to positively influence neurogenesis and vice versa. Neuroblasts tend to migrate towards areas were angiogenesis is strongly upregulated. Additionally, neuroblasts often migrate near blood vessels. However, NSC can also enhance angiogenesis through the expression of the pro-angiogenic protein VEGF.

1.3.4. Neurogenesis

Neurogenesis is a multistep process, which starts with the proliferation of the NSC residing in the subventricular zone (SVZ) of the lateral ventricles and the subgranular zone of the hippocampus (54). The regulation of neurogenesis is a dynamic process, meaning the number of newly formed neurons is highly dependent on the presence of environmental signals (55). The non-proliferating 'quiescent neural stem cell' (qNSC) at rest is activated when exposed to a variety of cues such as NOTCH1 signaling (56). Subsequently, it transforms into an activated NSC (aNSC), starts to proliferate and further evolves into a neural progenitor cell (NPC). These NPCs give then rise to the neuroblasts. At last, the neuroblast starts to migrate to the area of interest and differentiates into a neuron (57, 58). During maturation, the neuron develops neurite extensions, synaptic branches, and integrates into the surrounding neuronal circuits. However, only a small percentage of the newly formed neurons survives. 60-80% of the newborn cells will die during programmed cell death. This apoptosis is thought to be necessary to prevent dysfunctional signaling in the brain (59, 60).

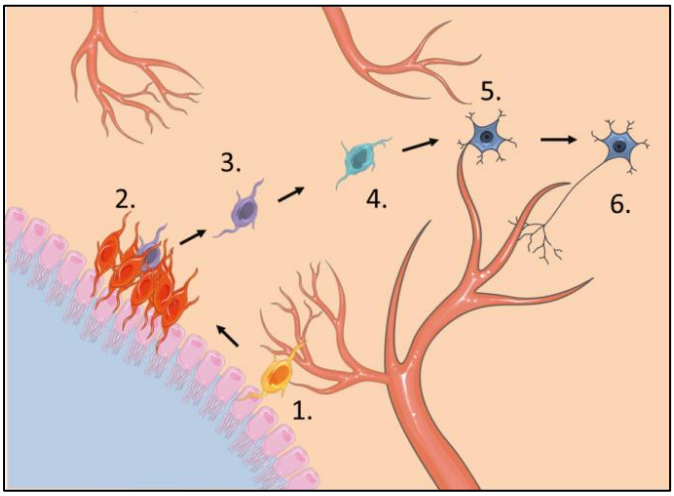

Figure 1: The process of neurogenesis starting in the SVZ. Neurogenesis starts with the qNSC, making contact with the blood vessels of the SVZ, being activated (1). Subsequently, the activated NSC starts to proliferate in the SVZ (2). Next, this NSC differentiates in a NPC (3). This cell type will further evolve in a neuroblast, which can to migrate towards the target area (4). Further, the neuroblast differentiates into an immature neuron and, neurite extensions will appear (5). At last, the neuron will fully mature, form synapses, and integrate itself into the neuronal circuits (6).

(The components of this figure were obtained from Sevier medical Art)

Under standard conditions, NSC proliferation and apoptotic rates are balanced, but during the ischemia of a stroke, proliferation is stimulated. Hence, more new mature cells are formed (61). It was suggested that stroke influences the neuronal phenotype by the up-regulation of several signaling pathways such as NOTCH, TNF -α, sonic hedgehog, and bone morphogenetic protein (62-64). Within the first two days post-stroke the cell cycle of the NSC is reduced to 11 hours. Together with a reduced division time, the switch from symmetric to asymmetric cell division is suggested to be involved in the increased NSC proliferation post-stroke. (51, 65). However, the natural increase in NSC proliferation and neurogenesis, in general, is limited and not sufficient to compensate for the enormous cell loss. Enhancement of this natural process may lead to effective therapies (see section 1.5.1). The neuroblasts formed during neurogenesis in the SVZ zone can to migrate towards damaged areas. This migration makes the SVZ an attractive target for such neurogenesis enhancing therapies (66). In mice, the appearance of neurogenesis in the SVZ after stroke is generally accepted. However, in humans, the occurrence of this phenomena is still controverting. Although confirming results exist, doubts if the occurrence of neurogenesis in the SVZ is only limited to the early postnatal development still live on (67-69).

1.4. Stem cell-based therapies

Stem cells are an up-and-coming tool for the development of new therapies. Several stem cell types are currently under investigation for the treatment of ischemic stroke.

1.4.1 Neural stem cells

Particularly interesting for the recovery of brain tissue is the NSC. For NSC-based therapies, two proposed approaches can be implemented. The first one is the enhancement of neurogenesis by stimulating the endogenous NSC compartment. The other one is by the transplantation of exogenous NSC to serve as a tissue-replacement therapy (70-72).

Exogenous NSC can be transplanted in the surrounding of the infarction. Differentiation of these stem cells into new neurons and the integration of these exogenous cells in the neuronal network is the desired result (73). Transplantation of NSC has been shown promising in animal models. Unfortunately, the isolation of NSC is challenging and the use of exogenous human NSC, as well as the harvesting, is paired with significant ethical problems (74, 75). These obstacles limit the therapeutic potential of exogenous NSC. However, the use of other stem cell sources such as mesenchymal stem cells (MSC) is not restricted by these ethical problems.

As previously mentioned, a potential approach is to stimulate the endogenous NSC compartment and as a result of this enhance endogenous neurogenesis to improve the formation of new fully integrated neurons. Several approaches have already been investigated. The administration of the p53 inhibitor Pifithrin-α, for example, is shown to promote NPC survival and functional improvement in rats (76). The administration of the trophic factor BDNF, as well as the practice of physical exercise, were able to stimulate neurogenesis animal models of stroke (77, 78). Physical exercise was even shown to counteract cognitive decline by upregulating neurogenesis in humans (79).

1.4.3. Mesenchymal stem cells

A stem cell type particularly appealing for the treatment of stroke is the mesenchymal stem cell (MSC); this interest is mainly devoted to its secretome. MSC can secrete a variety of paracrine factors, such as stromal derived factor 1 (SDF-1), brain derived neurotrophic factor (BDNF), VEGF, and IL-10 (80). This ability enables them to influence the neural environment after stroke. MSC are suggested to boost NSC migration and with this enhance neurogenesis, improve angiogenesis, and modulate the immune system after stroke (81-83). MSC can be found in a wide variety of tissues, for example, in the dental pulp. These stem cells can be easily extracted from the pulp of the third molars. Since this material can be non-invasively obtained, the use of human dental pulp stem cells (DPSC) is more favorable than other MSC sources such as bone marrow MSC. Several investigations revealing the therapeutic potential of DPSC in rodent stroke models have already been published (84, 85).

Because of their secretory capacities, the MSC is a favorable vehicle for the delivery of growth factors or chemokines. An interesting approach is to boost neurogenesis by the overexpression of a growth factor, together with the potent effects of the MSC secretome. BDNF and fibroblast growth factor 2 (FGF-2) overexpressing MSC, were seen to improve neurological recovery in a stroke animal model. BDNF improved synaptic plasticity, and FGF-2 had a positive effect on the proliferation of NPC (83, 86). The use of MSC is paired with another benefit. They are considered to be immuno-privileged, which can result in prolonged survival time *in vivo* compared to other cell types. The administration of these stem cells *in vivo* does, therefore, require no use of immunosuppressive agents, making them very useful (87). Based on these assumptions, it can be concluded that MSC possess the potential to be used for future ischemic stroke therapies.

1.5. Research plan

Previously our research group showed that human DPSC are significantly better in stimulating NSC migration then bone marrow MSC. Secretome analysis of DPSC (data not shown) was performed to identify the paracrine factors involved in NSC migration. Subsequently, a panel of possible migratory factors was tested with transwell migration assays and revealed recombinant insulin-like growth factor-2 (IGF-2) as a potent stimulator of NSC migration.

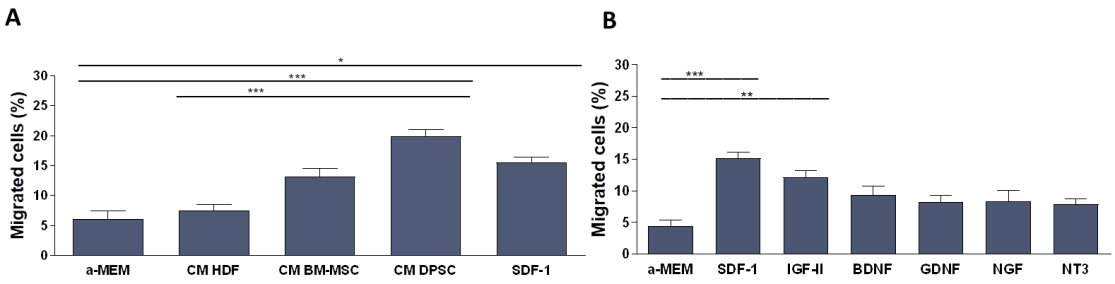

Figure 2: transwell migration of NSC towards conditioned media and selected panel of growth factors. (A) Migration of the NSC towards conditioned media of bone marrow MSC, DPSC ,and human dermal fibroblast (HDF) is tested. SDF-1 (+) and α-MEM medium(-) serve as controls.(*** P<0.001 * P< 0.05). **(B)** The migration towards a selected panel of growth factors present in the DPSC secretome. IGF-2, BDNF, glial cell-derived neurotrophic factor (GDNF), nerve growth factor (NGF), and neurotrophin-3 (NT3) were tested. SDF-1 (+), and α-MEM medium (-) served as controls. (*** P<0.001, ** P<0.01) *data was obtained by Yörg Dillen*

It is a growth factor that exerts a widespread panel of cellular effects, but the exact mechanisms and functions of this protein and its receptors have not yet been unraveled. IGF-2 is known to be of importance during survival, growth, and cellular development. IGF-2 even has a neuroprotective effect on cortical neuronal cultures under hypoxic conditions (88). This growth factor activates its pleiotropic effects by binding to the insulin-like growth factor-1 (IGF-1), IGF-2/mannose 6 phosphate receptor, and insulin receptors (88). Six insulin-like growth factor binding proteins (IGFBP) regulate IGF-2 and insulin-like growth factors (IGF) in general. Most of them have an inhibitory effect on the actions of IGFs. The growth factor array which was performed on the CM of human DPSC (data not shown) also revealed a high presence of IGFBP-6, while the other IGF binding proteins were present in much lower concentrations. IGFBP-6 is a well known IGF-2 inhibitor and has a higher affinity for IGF-2 than IGF-1 (84). To overcome these inhibitory effects, IGF-2 analogs were generated with a lower affinity for the IGFBPs. The engineered analogs Arg6 and Des[1-6] IGF-2 lack an IGFBP-binding site and are therefore less prone to IGFBP inhibition.

My study aim is to determine the neuroregenerative aspects of IGF-2-enhanced DPSC in ischemic stroke. As a result of this, I **hypothesize** that the selected IGF-2 analogs stimulate neurogenesis and angiogenesis *in vitro* and furthermore that transplantation of **IGF-2-enhanced human DPSC** in the distal middle cerebral artery occlusion mouse model enhances the endogenous neurogenesis and angiogenesis.

During this study, the objectives are to unravel the **migratory effects** of **IGF-2** and two engineered variants **Des[1-6]** and **Arg6 IGF-2** on NSC and endothelial cell migration, which is a process of great significance during neurogenesis and angiogenesis. Further, the migratory effects of these IGF-2 analogs will be compared after **inhibition with IGFBP-6**. The most potent variant will be selected to generate **a lentiviral DNA construct** that will be used for the transduction of DPSC. Additionally, it will be validated if DPSC are ideal stem cells to be used for an IGF-2-overexpressing cell line in ischemic stroke. By analyzing their IGF-2 secretory levels and confirming their ability to be successfully transplanted in a murine model of stroke.

2. Materials and methods

In the following sections, an overview of the experimental procedures performed during this study is given. With this, a detailed description of all the used materials and methods is provided.

2.1. Isolation and culture of human DPSC

Human DPSC were isolated utilizing the explant method as described by Hilkens et. al. The third molar teeth, removed for orthodontic reasons, were received from the hospital Oost-Limburg (ZOL). The donors (15-21 years of age) informed consent was given, and the use of the tissue donations was approved by the ethical committee of Hasselt University. After removal, the teeth were mechanically fractured, and the dental pulp was isolated from the tooth cavity. The pulp was rinsed in minimum essential medium, α-modification (α-MEM, Sigma-Aldrich, Saint-Louis, USA) which was supplemented with 10% fetal bovine serum (FBS, Biowest, Nuaille, France), 100 U/ml penicillin (Sigma-Aldrich), 100 µg/ml streptomycin (Sigma-Aldrich) and 2 mM L-glutamine (Sigma-Aldrich). Previously described medium can be referred to as DPSC standard medium. Next, the pulp was fragmented, and the tissue explants were seeded into 6-well plates (Greiner Bio-one, Kremsmünster, Austria) in DPSC standard medium. The explants were incubated at 37°C within a humidified atmosphere containing 5% CO_2. The medium was replaced every 3-4 days until 70-80% confluency was reached. Subsequently, the cells were harvested with 0.05% Trypsin/Ethylenediaminetetraacetic acid (EDTA, Sigma-Aldrich). Cryopreservation was performed in standard DPSC medium supplemented with 20% FBS, and 10% dimethyl sulfoxide (DMSO, Sigma-Aldrich), for sub-culturing cells were seeded at a density of $3x10^3$ cells /cm^2. Visualization was performed with the Nikon eclipse TS100 microscope (Nikon, Tokio, Japan) and progress capture pro software.

2.2. Culture of human microvascular endothelial cell culture

Human microvascular endothelial cells (HMEC-1) supplied by Gibco (Waltham, Massachusetts, USA) were cultured using MC DB 131 medium (Gibco) supplemented with 10% FBS, 10 mM L-glutamine, 100 U/ml penicillin, 100 µg/ml streptomycin, 1 µg/ml Hydrocortisone (Sigma-Aldrich), and 10 ng/ml epidermal growth factor (EGF, Gibco). The cells were incubated in a humidified atmosphere with 5% CO_2 at 37°C. The medium was replaced every 2-3 days, and the cells were trypsinized with 0,05% Trypsin/EDTA when 70-80% confluency was reached. The cells were re-seeded at a density of $3x10^3$cells /cm^2 until used for further experiments.

2.3. Isolation and culture of fetal mouse brain NSC

Neural stem cells were isolated from the embryos of pregnant mice (E13-15). The embryos were sacrificed by decapitation. The brains were isolated, submerged in 0.01 M phosphate buffered saline (PBS) supplemented with 100 U/ml penicillin, 100 µg/ml streptomycin and placed on ice. Next, the brains were minced and centrifuged for 8 min at 200 g. Subsequently, a solution containing 2 mg/ml collagenase A and 10 µg/ml DNase I dissolved in 0.01 M PBS was added to the brain samples and incubated for 1.5 hours at 37°C. Subsequently, the suspension was centrifuged at 300g for 5 min, the supernatant was removed, and the pellet was re-suspended in Neurobasal medium A (Gibco). This centrifugation and re-suspension step was repeated twice, during the last repetition the cells were re-suspended in neurobasal medium A supplemented with 2% B27 (without vitamin A, Life technologies, Waltham, VS), 2mM L-glutamine, 100 U/ml penicillin, 100 µg/ml streptomycin, 20 ng/ml EGF (Immunotools, Friesoythe, Germany), and 20 ng/ml FGF-2 (Immunotools). This medium may be referred to as the standard NSC culture medium. Subsequently, the fragments were flushed through a cell strainer (70 µm), and the suspensions were placed in T25 culture flasks. During the next 4-5 days, 20 mg/ml EGF and 20 mg/ml FGF-2 were supplemented every 2 days. Then the cell suspension containing neurospheres was centrifuged at 270 g for 5 min. Next, the cells were dissolved in accutase (Innovative cell technologies, inc. San Diego, USA) and incubated for 5 min at 37°C. The NSC were seeded at a density of $3x10^3$ cells/cm^2 in flasks coated with 5 µg/ml fibronectin dissolved in 0.01M PBS and incubated overnight at 37°C in a humidified atmosphere 5% CO_2. The NSC were passaged every 3-4 days with accutase when 70-80% confluency was reached and re-seeded at a density of $3x10^3$ cells /cm^2 until used for further experiments.

2.4. Culture of human dermal fibroblasts

HDF were purchased from Sigma-Aldrich and cultured on Dulbecco's modified eagle medium high glucose (DMEM, Sigma-Aldrich, Saint-Louis, USA) which was supplemented with 10% FBS, 100 U/ml penicillin, 100 µg/ml streptomycin. The HDFs were incubated in a humidified atmosphere containing 5% CO_2 at 37°C and were passaged every 6-7 days with 0.05% Trypsin/EDTA when 70-80% confluency was reached. The cells were reseeded at a density of $3x10^3$ cells/cm^2 until used for further experiments. For cryopreservation the medium was supplemented with 20% FBS and 10% DMSO.

2.5. Culture of bone marrow-derived mesenchymal stem cells

Bone marrow-derived mesenchymal stem cells (BM-MSC) were kindly provided by prof. Catherine Verfaillie and cultured within a humidified atmosphere at 37°C with 5% CO_2 in Dulbecco's modified eagle medium high glucose (DMEM, Sigma-Aldrich) which was supplemented with 10% FBS, 100 U/ml penicillin, 100 µg/ml streptomycin. The BM-MSC were trypsinized once every week with 0.05% Trypsin/EDTA when 70-80% confluency was reached and reseeded at a density of $3x10^3$ cells/cm^2. When cryopreserved the medium was supplemented with 20% FBS and 10% DMSO.

2.6. Immunocytochemistry with fluorescent detection method

NSC were seeded at a density of $3.2x10^3$ cells/cm^2 on glass coverslips in standard NSC culture medium. After two days incubation, the culture medium was removed, and the cells were washed with 0.01 M PBS. Subsequently, a fixation step using paraformaldehyde (PFA, 4%, Sigma-Aldrich) was applied for 20 min. Next, the cells were rinsed with 0.01 M PBS and incubated with 0.05% Triton-X-100 (Sigma-Aldrich) for 20 min. Subsequently, 10% protein block solution (Dako, Glostrup, Hovedstaden, Denmark) was applied and incubated for 30 min, followed by the administration of the primary antibody (*table 1*). After incubating overnight at 4°C the unbound antibodies were removed by rinsing the cells three times with PBS. Next, the secondary antibodies (*table 1*) were incubated for 30 min at room temperature and washed with PBS (3x). Cell nuclei were stained by incubation of 4',6-diamidino-2-phenylindole (DAPI) for 10 minutes. The coverslips were mounted on glass slides using Fluoromount-G mounting medium (Invitrogen). Analyzation of the histological slides was performed with a Leica DM 4000 BLED fluorescent microscope (Leica, Wetzlar, Germany) using Leica application suit X software.

2.7. Immunohistochemistry

The paraffin embedded brain slices of mice brains with a permanent distal middle cerebral artery occlusion were deparaffinized by submerging the slides in xylol, following hydrating them in a serial dilution of ethanol (100%, 95%, 80%, and 70% ethanol), and rinsing them using 0.01 M PBS. For the diaminobenzidine (DAB) detection method, peroxidase block (Dako) was administered for 30 min. Optionally, antigen retrieval with citrate buffer pH 6 was used (microwave for 2 min at 800W, following 3 min at 480 W and 45 min of cooling down) and/or a 30 min incubation with 0.05 % Triton-X-100 was applied. Subsequently, the primary antibodies (*table 1*) were incubated overnight at 4°C and as a negative control, an isotype antibody (*table 1*) was used. The unbound anti-bodies were washed away by rinsing the slides with 0.01M PBS (3x), and the secondary antibodies (*table 1*) were administered for 30 min at room temperature.

2.7.1. Immunofluorescent detection

During fluorescent detection, the secondary-antibodies were conjugated with Alexa Fluor® 555 (Invitrogen) molecules. To indicate the presence of cell nuclei, a counterstaining was achieved by the incubation of DAPI (10 min). Next, mounting of the coverslips was performed using Fluoromount-G mounting medium. Further analysis was performed with a Leica DM 4000 BLED fluorescent microscopy using Leica application suit X software (Leica).

2.7.2. Diaminobenzidine immunodectection

The DAB detection required the use of horseradish peroxidase (HRP) labeled antibodies. After binding of the secondary antibody, the DAB substrate kit (Dako) was applied to indicate the presence of HRP-labeled antibodies. After rinsing the slides in distilled aqua, a counterstaining with hematoxylin (5 min) was performed. Subsequently, the slides were placed under a continues flow of tap water for 5 min. At last, the tissue slices were dehydrated in ethanol (70%, 80%, 95%, and 100% ethanol) and submerged in xylol. Mounting of the coverslips occurred with DPX mounting medium and analysis was performed with the Nikon Eclipse 80i microscope (Nikon) and NIS Elements BR 3.10 software.

Table 1: Antibodies Immunostainings

Target	Conjugate	Host	Dilution	Supplier, Ref number
Primary antibodies				
GFAP	_	***goat***	***1:400***	***Santa Cruz Biotechnology, sc-6170***
SOX2	_	***rabbit***	***1:1000***	***Abcam, Ab97959***
EGFR	_	***rat***	***1:200***	***Abcam, ab231***
CD133	_	***rabbit***	***1:50***	***Abcam, ab16518***
PSA-NCAM	_	***mouse***	***1:100***	***Thermo Fisher, 14-9118-82***
βIII-tubulin	_	***mouse***	***1:2000***	***Sigma-Aldrich, T8578***
Map2	_	***rabbit***	***1:1000***	***Abcam, ab32454***
NeuN	_	***mouse***	***1:50***	***Millipore, MAB377***
DCX	_	***rabbit***	***1:250***	***Abcam, ab207175***
Vimentin	_	***mouse***	***1:500***	***Dako, M0725***
IBA-1	_	***rabbit***	***1:400***	***Wako, 019-19741***
Secondary antibodies				
Mouse IgG	***HRP***	***Goat***	***RTU***	***Dako, K4007***
Mouse IgG	***AF555***	***Goat***	***1:500***	***Invitrogen, A21425***
Rabbit IgG	***AF555***	***Goat***	***1:500***	***Invitrogen, A21430***
Rat IgG	***AF555***	***Goat***	***1:500***	***Invitrogen, A21434***
Goat IgG	***AF555***	***Donkey***	***1:500***	***Invitrogen, A21432***
Isotype antibodies				
Mouse IgG1,K	_	***Mouse***	_	***R&D systems, MAB002***
Rabbit IgG	_	***Rabbit***	_	***Abcam, ab172730***
Rat IgG2A	_	***Rat***	_	***R&D systems, MAB006***
Goat IgG	_	***Goat***	_	***R&D systems, AB-108-C***

Santa cruz biotechnology, Dallas, Texas, USA
Abcam, Cambridge, United Kingdom
R&D systems, Minneapolis, USA
Invitrogen, Carlsbad, California, USA

2.8. Propidium iodide cell survival assay

To evaluate the NSC proliferation, a propidium iodide cell survival assay was utilized. With this assay $3x10^4$ cells/well were seeded in a black 96 well plate (Greiner Bio-one) diluted in α-MEM (Sigma-Aldrich) supplemented with 1% B27 (Life Technologies), 10 ng/ml EGF and 10 ng/ml FGF-2. After incubating 4 hours, baseline measurements were made. For each well, the culture medium was removed and replaced by 75 µl Lysis buffer A100 (Chemometec, Lillerod, Denmark). After a 5 min during incubation, 75 µl stabilization buffer (Chemometec) and 3 µl propidium iodide (Chemometec) were added. Next, the cells were incubated for 15 min in a dark surrounding. Then the fluorescence intensity was measured with an automated microplate reader (BMGlabtech, Ortenberg, Germany) at an excitation wavelength of 540 nm, an emission wavelength of 612 nm, and a gain of 2000x. After base measurements, the cells were placed on different experimental conditions. As negative control α-mem supplemented with 1% B27, 10 ng/ml EGF and, 10 ng/ml FGF-2 was used. To the experimental conditions 1 ng/ml and 100 ng/ml IGF-2 were added. As a fourth experimental condition DPSC conditioned medium made in α-MEM supplemented with 1% B27, 10 ng/ml EGF and, 10 ng/ml FGF-2 was used. Subsequently, fluorescence intensity measurements were taken at 24 and 48 hours.

2.9. Transwell migration assay of NSC

The migratory properties of NSC towards wild type IGF-2 (Gropep, Thebarton, Australia) and the IGF-2 variants Des[1-6] (Gropep), and Arg6 (Gropep) were examined using a transwell migration assay. Furthermore, increasing IGFBP-6 (R&D systems) concentrations were added to 1 ng/ml of the three IGF-2 variants to evaluate the inhibitory effect of IGFBP-6. The set-up contained 24-well plates (Greiner Bio-one) inserted with transwells (8 µm pore size, Greiner Bio-one). The inserts were coated with 5 ng/ml fibronectin (R&D systems) and incubated overnight at 37°C. Subsequently, NSC were seeded at a density of $5x10^4$ cells/insert in 150 µl of α-MEM supplemented with 0.2% B27 (without vitamin A), 10 ng/ml EGF, and 10 ng/ml FGF-2. Migration was tested towards a panel of different conditions by adding 500 µl of the experimental condition to the lower compartment of the well. After an incubation period of 24 h, the cells were fixed using 4% PFA during 15 min and stained with 0.1% crystal violet for 30 min. The un-migrated cells located at the upper side of the membrane were removed by wiping them with a cotton swab, and the migrated cells were visualized with the Nikon Eclipse TS100 microscope and progress capture pro software. Quantification of the migrated cells occurred by measuring the area percentage of migrated cells with Axiovision software.

For the first pilot experiment migration towards IGF-2, Arg6 IGF-2, and Des[1-6] IGF-2 was tested at concentrations of 1 ng/ml and 100 ng/ml. A-mem was used as a negative control. Secondly, an experiment to test migration in attendance of the IGF-2 inhibitor IGFBP-6 was performed. Migration towards 1 ng/ml IGF-2, Arg6 IGF-2, and Des[1-6] IGF-2 was tested at elevating concentrations of IGFBP-6 (1 ng/ml, 10 ng/ml, 100 ng/ml and 1000 ng/ml) as positive control

migration towards IGF-2, Arg6 IGF-2, and Des[1-6] IGF-2 without IGFBP-6 administration was tested.

2.10. Transwell migration assay of HMEC-1

To indicate the pro-angiogenic properties of IGF-2 and the IGF-2 variants Des[1-6], and Arg6, migration of HMEC-1 were tested. The set-up contained 24-well plates inserted with transwells (8 µm pore size). Subsequently, Human microvascular endothelial cells were seeded in the upper well at a density of $1x10^5$ cells/insert in 150 µl α-mem supplemented with 0.05% FBS. Migration was tested towards a panel of different conditions which were added to the lower well (500 µl). IGF-2 and IGF-2 variants Des[1-6], and Arg6 were tested at different concentrations (1 ng/ml, 10 ng/ml and 100 ng/ml). As negative and positive control α-mem supplemented 0.05% FBS (-) and 10% (+) were used. After an incubation period of 24 h, the cells were fixed using 4% PFA during 15 min and following stained with 0.1% crystal violet for 30 min. The un-migrated cells located at the upper side of the membrane were removed by wiping them with a cotton swab. Pictures were taken with the Nikon Eclipse TS100 microscope and progress capture pro software and the area percentage of migrated cells was quantified Axiovision software.

2.11. Permanent dMCAO mice model

To induce a focal ischemic lesion in mice, the permanent distal middle cerebral occlusion (dMCAO) model was applied on male C57BL/6J mice (10 weeks old). Herewith, the distal middle cerebral artery (dMCA) at the left hemisphere is coagulated proximally to the bifurcation. Briefly, the mice were anesthetized using 2% isoflurane. Next, they were placed on a heating mat to maintain the body temperature at 36,5 °C. Vet ointment was applied to the eyes to protect the mice from eye dryness. Then an incision was made, between the eye and ear of approximately 1 cm. Subsequently, the skin and temporal muscle were removed, and the temporal bone was thinned with a small drill until the dMCA could be exposed. The skull was removed at the site of the MCA, and the meninges were carefully dissected to expose the dMCA. The dMCA was occluded by means of electrocoagulation proximally to the bifurcation. The incision was sutured with a monofilament nylon suture (7-0). The mice received 0.05 mg/kg buprenorphine subcutaneously for analgesia and were placed in a recovery chamber (32 °C).

To validate the lesion size induced by the permanent dMCAO model, a 2,3,5-Triphenyl-tetrazolium chloride (TTC, Sigma-Aldrich) solution was used. It enables the indication of metabolic activity (in red) and metabolic inactivity (in white). For the TTC assay, six mice were sacrificed through cervical dislocation. Subsequently, the mice brains were isolated and divided into 1 mm thick frontal slices. The slices were placed in 20 mg/ml TTC solution diluted in 0.01 M PBS. After 30 minutes, the tissue samples were visualized and scanned using a multifunction printer. Quantification occurred with ImageJ software. With this application, the surface area of the contralesional hemisphere (= C_i) and the ipsilesional hemisphere without the infarcted area (= N_i) were measured. Following the formula of Lin et al. (infarct volume (%) = $(\sum_i(C_i-N_i)/(\sum_i C_i))*100$)

the infarcted volume % of the ipsilesional hemisphere was calculated (89). Of each mice brain, the six brain slices were measured to calculate the infarcted volume %.

2.12. GFP-DPSC transplantations in dMCAO mice

Two administration methods were tested to determine the optimal transplantation site for DPSC injections in dMCAO mice, namely intra-cerebroventricular (ICV) and perilesional (PL). For this animal experiment, 12 mice were used. First a permanent focal ischemia was induced by means of the dMCAO model as previously explained. 48h later the green fluorescent protein (GFP) transduced human DPSC were injected by stereotactic injection. For the PL injections, a total of $5x10^4$ cells were injected diluted in 1 µl 0.01M PBS. The injection was performed in two times, in the first injection, 0.5 µl is injected in the putamen, and after pulling back the needle slightly again, 0.5 µl is injected in the cortex. The coordinates of PL injection were A/P: 0.00mm, M/L: -2.00 mm and D/V: -2.50 mm first and -1.75 mm for the second injection. During the ICV injections $1,5x10^5$ cells diluted in 2 µl PBS were injected at the coordinates A/P: 0.00 mm, M/L: -1.00 mm and D/V -2.2 mm. Injection rate for both injections was 0.5 µl/min. The first six mice were injected in the lateral ventricles; the second half was injected perilesional. One day after transplantation, three mice of each group were sacrificed. Seven days after transplantation, the other six mice were sacrificed. The mice were perfused with Ringer solution containing 4% paraformaldehyde, and the brains were embedded in paraffin for immunohistochemical analysis.

2.13. Sub-cloning of IGF-2 and Des[1-6] IGF-2 in a lentiviral plasmid.

In order to obtain a recipient plasmid containing the desired Des[1-6] IGF-2 analog or wild-type IGF-2 required to generate a lentiviral vector; the IGF-2 and Des[1-6] IGF-2 fragments purchased from IDT first had to be amplificated to produce a stock solution required for further use. Using the pBAD/TOPO™ Thiofusion ™ expression kit, a supply of IGF-2 and Des[1-6] IGF-2 containing pBAD/TOPO™ constructs was generated.

Subsequently, IGF-2 and IGF-2 Des[1-6] TOPO vectors were digested with FastDigest MreI (ThermoFisher) and FastDigest NheI (ThermoFisher). Simultaneous, the recipient plasmid was exposed to the same restriction enzymes. The recipient plasmid, a lentiviral DNA construct containing EF1a-HSVtk-Fluc (*Figure 3*), was kindly provided by the research group of Prof. dr. Esther Wolfs. The reaction occurred in the compatible FastDigest green reaction buffer (ThermoFisher) at 37°C for 30 min. After that, the digested samples were maintained at 4°C until parted with gel electrophoresis (1% agarose). After running for approximately 60 min at 120 eV the demanded plasmid without the HSV-tk gene (removed by restriction digestion) and the IGF-2, Des[1-6] IGF-2 DNA samples were isolated trough extraction with the PCR clean-up kit (Qiagen, Hilden, Germany). Next, a DNA ligation was conducted with T4 ligase (Thermo Fisher) and the compatible T4 buffer to fuse the IGF-2 and plasmid backbone. The reaction occurred at 22°C for two hours followed by a (10 min during) deactivation step at 65°C.

Next, the ligated plasmid was amplified through transformation in NEB® 5-alpha competent E. coli (New England Biolabs). Ensuing, the E. coli bacteria, thawed on ice, were incubated for 30 min. on ice together with the ligation product. A heat shock of 30 sec followed the previous step at 42°C after which the samples were placed on ice again for 5 min. Subsequently, SOC-medium was added, and the bacteria were shaken for 1 hour (250 rmp, 37°C) and plated out on LB agar medium supplemented with 1 µg/ml ampicillin (Sigma-Aldrich) an incubated overnight at 37°C. The single colonies which occurred on the plates were picked and placed overnight on LB Broth medium supplemented with ampicillin. The ligated plasmids were extracted from the bacteria and purified utilizing the Nucleospin® Plasmid EasyPure kit (Macherey-Nagel, Düren, Germany). To validate if a correct ligation occurred, the plasmids were again restricted with BamHI and separated with 1% gel electrophoresis.

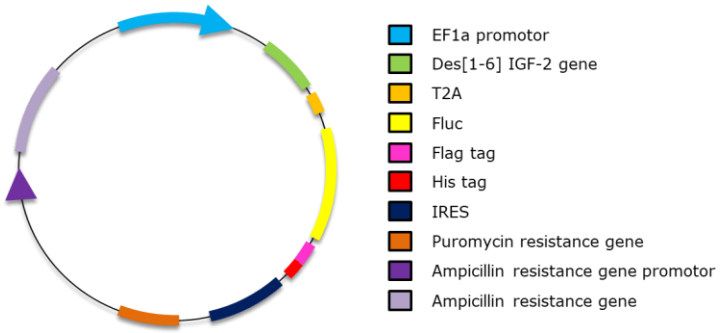

Figure 3: Lentiviral DNA construct. The lentiviral DNA construct received from the research group of Prof. dr. Esther wolfs contained a human elongation factor-1 alpha promoter (EF1α promoter) followed by a HSV-tk gene, a thosea asigna virus 2A (T2A) self-cleaving sequence, an firefly luciferase gene (Fluc), a Flag and His tag, an internal ribosomal entry site (IRES), and a puromycin and ampicillin resistance gene.

2.14. ELISA of IGF-2

To analyze the IGF-2 secretion levels of DPSC, BM-MSC and HFD, conditioned medium (CM) was made. This was obtained by seeding cells $2x10^4$ cells/cm^2 on (1 ml/$4x10^3$ cells) DMEM supplemented with 10% FBS, 100 U/ml penicillin, 100 µg/ml streptomycin. After 24 h , the cells were washed 3x with 0.01M PBS and placed for 48 h on serum-free medium. After 48 h, the CM was removed and filtered (0.22 µm filter). The IGF-2 concentration of the conditioned media was measured using a Quantikine® enzyme linked immunosorbent assay (ELISA) (R&D systems) kit according to the manufacturers' protocol. With this, the IGF-2 concentrations were calculated based on the measured OD value at 450 nm.

2.15. statistics

For statistical analysis of the required data the program graphpad 8 was used. The aquired data were presented as mean and standard error of the mean (mean±SEM). To test for normality the D'agostino & Pearson test was applied. When the data was normally distributed a one-way ANOVA was applied combined with a Tukey multiple comparison test. In case of no normality the Friedman test was used for paired data and the Kruskal-Wallis for unpaired data. Both were combined with a Dunn's post hoc comparison. (*P< 0.05 , **P< 0.01, ***P<0.001)

3. Results

The next paragraphs contain an overview of the results obtained during this study. On the following pages, the migratory properties of NSC and HMEC-1 towards IGF-2 and two IGF-2 engineered variants, Des[1-6] and Arg6, are investigated. Further, the isolated NSC used during *in vivo* experiments are characterized. Next, an IGF-2 and a Des[1-6] IGF-2 containing lentiviral DNA construct is generated, to obtain an IGF-2-enhanced DPSC-cell line. Moreover, dMCAO mice model for ischemic stroke is validated, and a comparing analysis of two stereotactic injection methods for DPSC transplantations in ischemic stroke is made.

3.1. Isolation of DPSC

DPSC used during this study are obtained from the pulp of third molar teeth. The extracted third molars of this patient (patient number 188) are variable in size and stage of development (*figure 4A*). With the explant method, DPSC cells are cultured out of the fractionated dental pulp. The explant (*figure 4B*) shows outgrow of DPSC. At higher magnification (*10x, figure 4C*), the morphological characteristic of the DPSC can be visualized. The DPSC in culture have a typical polygonal or fibroblast-like shape, are bipolar or multipolar and adhere to plastic surfaces.

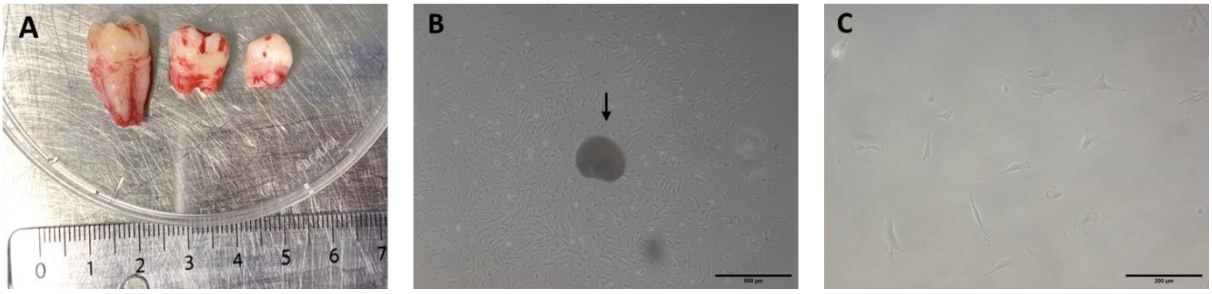

Figure 4: Extraction and isolation of DPSC. (A) Third molar teeth, extracted from patient 188, used for isolation of DPSC. **(B)** The dental pulp explant shows outgrow of DPSC, as indicated by the arrow (magnification 4x). **(C)** Magnification 10x shows the typical polygonal and fibroblast-like shaped cells in a DPSC cell culture. (Scale Bars: A= 7 cm, B= 500 µm, and C= 200 µm)

3.2 IGF-2 production by DPSC

The IGF-2 secretion of DPSC was analyzed by means of an ELISA and compared with HDF and BM-MSC (*figure 5*). After analysis, DPSC (175.3 ± 18.35) revealed to produce a larger amount of IGF-2 than the BM-MSC (131.4 ± 4.62), and even significantly more than the HDF (117.6 ± 3.18).

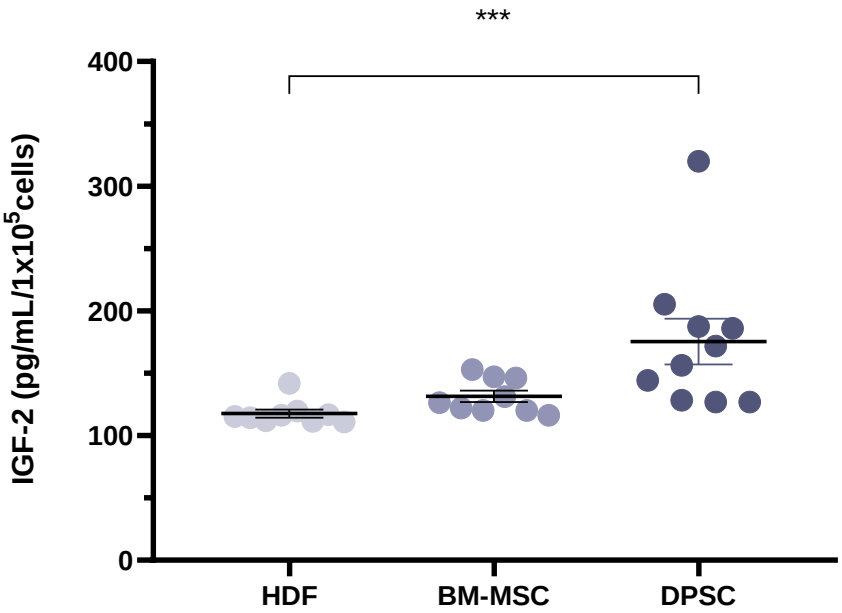

Figure 5: DPSC produce more IGF-2 then BM-MSC and HDF. The concentrations of IGF-2 in HDF, BM-MSC and DPSC were measured by means of an ELISA. DPSC (175.3 ± 18.35) produce significantly more IGF-2 then HDF (117.6 ± 3.18) (***P<0.001, N=9 for HDF and BM-MSC, and N=10 for DPSC, Kruskal-Wallis test with Dunn's multiple comparison)

3.3. The migratory effects of IGF-2 on NSC

An NSC culture, originating from isolated mice brain, was started to evaluate the migratory effects of NSC towards the IGF-2 analogs Des[1-6] and Arg6 *in vitro*. Before an analysis of the migratory effects with transwell migration assay could be performed, the NSC in culture first had to be characterized.

3.3.1. Characterization of NSC culture

To evaluate the expression profile of the NSC culture used for *in vitro* experiments, a panel of NSC and neuronal markers was tested (*figure 6*). Employing immunocytochemistry the presence of the markers SRY (sex determining region Y)-box 2 (SOX2), CD133, epidermal growth factor receptor (EGFR), doublecortin (DCX), polysialylated-neural cell adhesion molecule (PSA-NCAM), glial fibrillary acidic protein (GFAP) and β3-tubulin was determined. The NSC have a distinct expression of SOX2, CD133, DCX, and EGFR. However, PSA-NCAM, GFAP, and β3-tubulin positive cells are not detected.

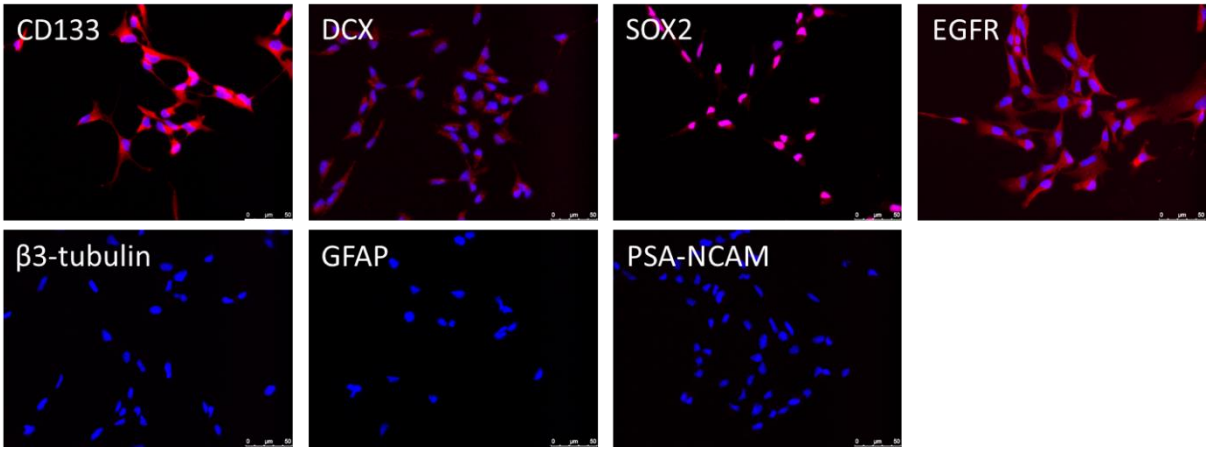

Figure 6: Expression profile of NSC culture. The NSC culture analyzed with immunocytochemistry showed expression of CD133, EGFR, SOX2 and DCX. The cells were negative for β3-tubulin, GFAP, and PSA-NCAM. (Magnification 40x and scale bar=50 µm)

3.3.2. NSC migration towards IGF-2 and the IGF-2 analogs Des[1-6] and Arg6

To assess the properties of the IGF-2 analogs, Des[1-6] and Arg6, on NSC migration, a transwell migration assay was performed. Migration towards IGF-2 and the two analogs at a concentration of 1 ng/ml and 100 ng/ml was tested during a pilot experiment (*figure 7*). A-mem medium served as a negative control. After crystal violet staining the migratory effects of IGF-2 were demonstrated. Quantification of the area percentage of migrated cells shows that wild type IGF-2 (37.54% ± 5.55%) and the engineered variants Des[1-6] (37.05% ± 5.80%) and Arg6 (38.34% ± 5.00%) stimulate NSC migration compared to the negative control (8.71% ± 1.18%) at a concentration of 1 ng/ml IGF-2. At a concentration of 100 ng/ml, IGF-2 shows a similar level of NSC migration.

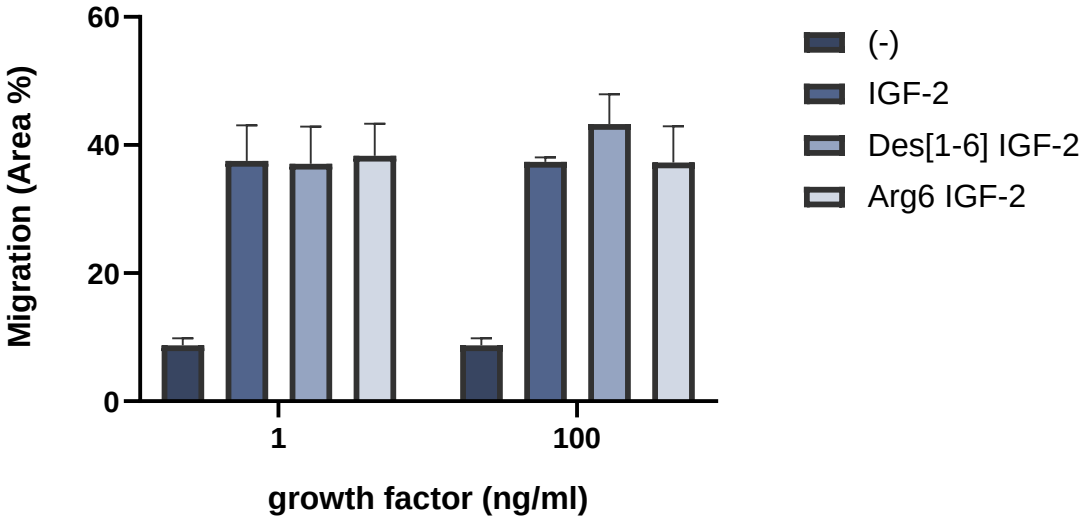

Figure 7: NSC migrate towards IGF-2 and IGF-2 variants Des[1-6] and Arg6. The effect of 1 ng/ml and 100 ng/ml IGF-2 and IGF-2 analogs Des[1-6] and Arg6 on NSC migration was investigated by transwell migration assay. After 0.1% crystal violet staining, the area percentage of migrated NSC was measured. IGF-2 (37.54% ± 5.55%) and IGF-2 variants Des[1-6] (37.05% ± 5.80%) and Arg6 (38.34% ± 5.00%) generate more NSC migration compared to the negative control α-mem (-) (8.71% ± 1.18%) at a concentration of 1 ng/ml. At 100 ng/ml again the IGF-2 analogs and IGF-2 generate visibly more NSC migration than the negative control. (N=3)

3.3.3. NSC migration towards IGF-2 and the IGF-2 variants Des[1-6] and Arg6 with IGFBP-6 inhibition

A transwell migration assay was performed, to reveal if the engineered IGF-2 variants are less prone to inhibition of IGFBP-6 (*figure 8*). NSC migration towards 1 ng/ml growth factor was tested in combination with an elevating concentration of IGFBP-6 (1 ng/ml, 10 ng/ml, 100 ng/ml and 1000 ng/ml). As positive control, an experimental condition with 0 ng/ml IGFBP-6 was used. After quantitative analysis of the area percentage of migrated cells, the percentage compared to the positive control (IGFBP-6 0 ng/ml) control was calculated. At a concentration of 100 ng/ml IGFBP-6, the analogs Des[1-6] (85.21% ± 3.07%) and Arg6 (88.67% ± 8.97%) show more NSC migration then wild type IGF-2 (31.15% ± 3.47%) and are therefore less inhibited by the IGFBP-6 administration. The Arg 6 variant shows even significant more migration (**<0.01). However, at a higher concentration of 1000 ng/ml, IGFBP-6 is able to reduce the migration of NSC in all conditions, indicating that the variants can also be inhibited by IGFBP-6.

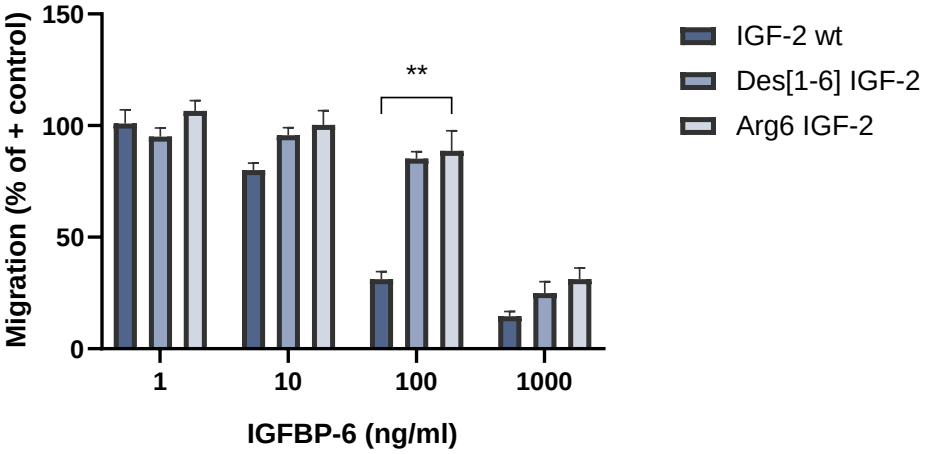

Figure 8: IGFBP-6 inhibits migration of IGF-2 and IGF-2 variants Des[1-6] and Arg6. The IGF inhibitor IGFBP-6 inhibits migration of NSC induced by IGF-2 (1 ng/ml IGF-2) at elevating concentrations of IGFBP-6 (1 ng/ml, 10 ng/ml, 100 ng/ml, and 1000 ng/ml)**.** Migration was measured as area % and set as % of the positive control which was 1 ng/ml IGF-2 with 0 ng/ml IGFBP-6. At a concentration of 100 ng/ml IGFBP-6 the IGF-2 variants Arg6 (88.67% ± 8.97%) and Des[1-6] (85.21% ± 3.07%) show to have significantly more migrated cells then the wild type IGF-2 (31.15% ± 3.47%). The data were represented as mean and standard deviation. For statistical analysis, the Friedman test with Dunn's multiple comparisons was applied. (N=5, **P<0.01)

3.3.4. Validation of NSC migration by means of cell survival

To determine whether the NSC migration, which was previously detected, was valid and not caused by proliferation induced by IGF-2; a propidium iodide cell survival assay was performed (*figure 9*). During this experiment, similar experimental conditions as used during the transwell migration assay were tested. Cell survival on 1 ng/ml IGF-2, 100 ng/ml IGF-2, and a-mem (negative control) were the experimental conditions. The CM of DPSC was also tested. The baseline measurement of the fluorescence intensity was made 4 hours after seeding the cells. Consequently, 24 h and 48 h later the fluorescence intensity was measured to estimate the DNA content in the different conditions (*figure 9*). The increase in DNA content (equalized to an increase in fluorescence intensity) indicates an increase in cell count and thus, proliferation. At 24 hours a slight increase in DNA content is detected on α-mem medium, suggesting a small proliferative effect. With the other conditions the DNA content decreases after 24 h suggesting less cells are present. At 48 h the DNA content is decreased on all conditions, with the IGF-2 and CM up to 50% lower than the baseline measurement.

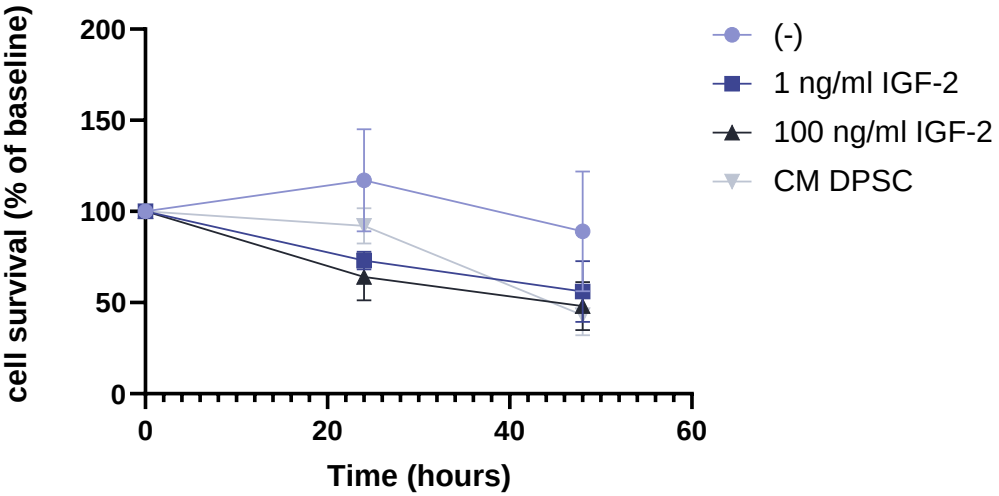

Figure 9: Administration of IGF-2 and DPSC CM has no proliferating effect on NSC. The proliferative effects of IGF-2 1 ng/ml and 100 ng/ml and CM of DPSC on NSC were tested with a propidium iodide assay. A-Mem served as negative control (-) and as baseline measurement the fluorescence intensity was measured 4 h after seeding the cells. The percentage of fluorescence intensity of the baseline measurement is calculated at 24 h and 48 h, indicating proliferation when exceeding the baseline value. For all conditions, except the negative control, a decreasing trend in DNA content is observed. (N=3)

3.4. The migratory effects of IGF-2 on HMEC-1

Neurogenesis and angiogenesis go hand in hand (51). To investigate whether the IGF-2 analogs also affect angiogenesis, their effect on endothelial cell migration, one of the key steps in angiogenesis, was also assessed.

Migration was tested towards an elevating concentration (1 ng/ml, 10 ng/ml and 100 ng/ml) IGF-2, Des[1-6] IGF-2 and Arg6 IGF-2. As controls α-mem supplemented with 0.05% (-) and 10% (+) FBS were applied. Quantification of the area percentage of migrated cells resulted in a significant outcome. The two IGF-2 analogs and the WT IGF-2 were all able to generate HMEC-1 migration. The WT IGF-2 and Des[1-6] IGF-2 show to generate significantly more migration than the negative control at a concentration of 100 ng/ml (*figure 10*). However, at lower concentrations of IGF-2, no acceptable difference is detected.

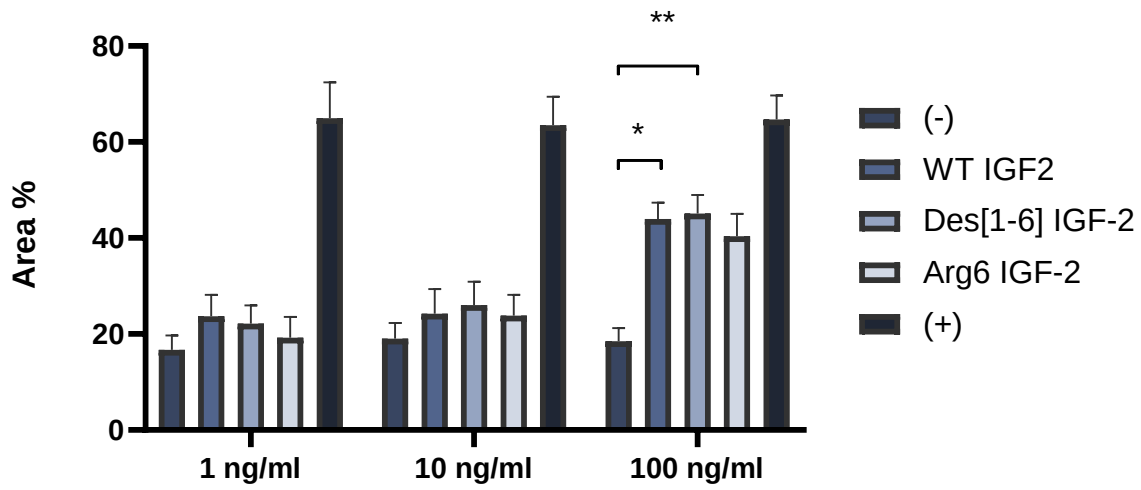

Figure 10: IGF-2 and IGF-2 analogs Des[1-6] and Arg6 generate migration of HMEC-1. The effect of 1 ng/ml and 100 ng/ml IGF-2 and IGF-2 analogs Des[1-6] and Arg6, on HMEC-1 migration, was investigated by transwell migration assay. After 0.1% crystal violet staining, the area percentage of migrated HMEC-1 was measured. At 100 ng/ml the IGF-2 analog Des[1-6] and WT IGF-2 generate significantly more HMEC-1 migration than the negative control. For the 1 ng/ml N=4, 10 ng/ml N=5 , and 100 ng/ml N=6. (*P<0.05 and **P<0.01)

3.5. Construction of an IGF-2 and Des[1-6] IGF-2 lentiviral plasmid

To produce an IGF-2 overexpressing DPSC line; a lentiviral vector has to be obtained. First a transfer plasmid containing the transgene of interest IGF-2 or Des[1-6] IGF-2 had to be created. A plasmid (*figure 3*) containing a firefly luciferase gene was used as a backbone and ligated with the Des[1-6] IGF-2 gene and the wild-type IGF-2 gene through sub-cloning. To control for correct ligation a restriction digestion with BamHI was performed. After separating the restricted fragments (*figure 9*) the expected fragment of 2087 BP for the Des[1-6] IGF-2 plasmid (Des[1-6] IGF-2 + Fluc genes) and 2105 BP for the IGF-2 plasmid (IGF-2 + Fluc genes) are detected as well as a light fragment of the remaining plasmid 7528 BP indicated by the black arrows (*figure 11*). Meaning both the IGF-2 DNA fragments are cloned in the transfer plasmid. However, besides the expected fragments, another fragment at the height of more or less 4800 base pairs (BP) is visible.

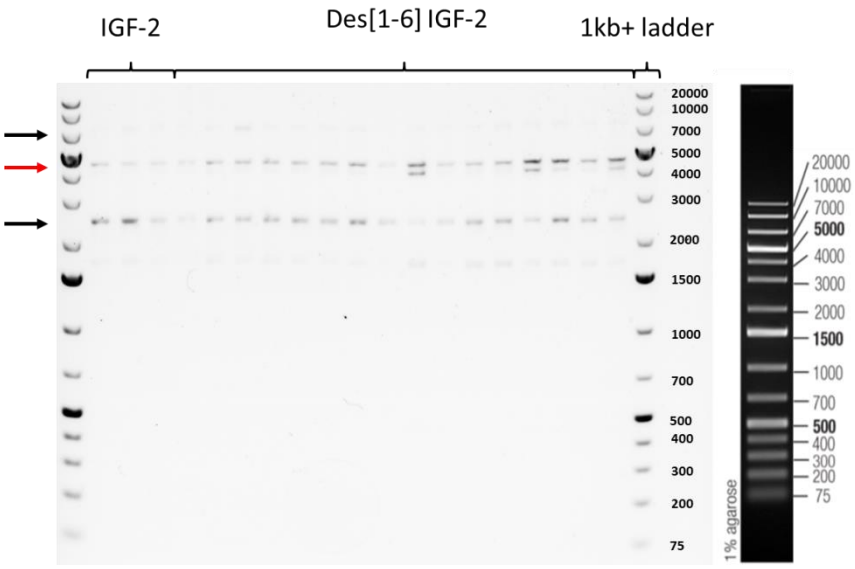

Figure 11: Restriction digestion of IGF-2 and Des[1-6] IGF-2 lentiviral plasmid. After restriction digestion of IGF-2 and Des[1-6] IGF-2 lentiviral plasmid with BamHI the expected fragment of 2087 BP for the Des[1-6] IGF-2 plasmid (Des[1-6] IGF-2 + Fluc genes) and 2105 BP for the IGF-2 plasmid (IGF-2 + Fluc genes) were visible (black arrow). The black arrow indicates the remaining plasmid at the correct height of 7528 BP. At +/- 4800 BP, an unexpected fragment was detected (red arrow). (Agarose gel electrophorese 1% and 1kb+ ladder)

3.5. Optimization of stereotactic DPSC transplantation in dMCAO mice model

Optimizing the mode of administration is required to maximize the effects of IGF-2 DPSC transplantation in the stroke model. Therefore, the following experiments show the validation of a stroke model and the optimization of stereotactic DPSC transplantations.

3.5.1 Validation of the dMCAO model

To simulate an ischemic event and generate a stroke lesion; the distal middle cerebral artery occlusion model was applied. Using a TTC staining a distinction between the lesion and healthy tissue could be made in brain slices obtained 48 h after stroke induction. Lesions are detected in the cortex of each mouse (*figure 12 A*). The lesions are always situated on the left hemisphere were the occlusion was created and the lesion border is continuously positioned above the corpus callosum. Quantification of the mice brain (n=6) reveals the average lesion size of the occluded hemisphere is 14.79% and with a standard error of the mean of 3.52% (*figure 12 B*).

Figure 12: Validation of dMCAO model with TTC assay. (A) With TTC, the presence of a stroke lesion was indicated in distal middle cerebral artery occluded (dMCAO) mice. **(B)** The average infarct volume (14.79% ± 3.52%). The infarct volume of the sick hemisphere of each mouse is calculated. (N=6)

3.5.2 Comparison of DPSC transplantation methods

In order to obtain the optimal mode of administration to transplant DPSC in the dMCAO stroke mice model, two injection methods are tested and compared. The transplantation of DPSC in the PL area and injection in the lateral ventricles were compared. It was evaluated if DPSC could be successfully transplanted and whether they were able to survive for at least seven days. The DPSC used during this experiment were transduced with a green fluorescent protein gene, which enables tracing DPSC in tissue samples.

To indicate the presence of the stroke lesion; an immunohistochemical analysis of neuronal nuclei (NeuN) was performed (*figure 13*). This analysis provides information about the lesion size and shape. The presence of NeuN was indicated with a red fluorescent signal. Within the area, expected to be the stroke lesion, the neuronal nuclei present a different cell morphology. Overall they are smaller and possess a more polygonal shape compared to the other neuronal nuclei in the surrounding brain areas. A border on which morphological changes occur is perceived, which is indicated with a dashed line (*figure 13*). The neuronal nuclei which are not situated within this indicated area possess round nuclei and had more NeuN expression.

To determine if DPSC transplantations with both injection methods were successful and to check for correct positioning of the stem cells relative to the stroke lesion; an analysis was performed on six mice sacrificed one day after DPSC transplantation (*figure 13*). After both the ICV and PL injections, GFP-positive cells are detected. In the ICV injected mice, green fluorescent cells are visible in the lateral ventricle (*figure 13 A-C).* The cells form a green globular cluster, present in the later ventricle, near the ischemic border. In the mice with PL transplanted DPSC (*figure 13 D-F)*, green fluorescent cells are detected next to the ischemic border. The cells are more diffusely spread in the perilesional area, compared to the clustered cells in the lateral ventricles.

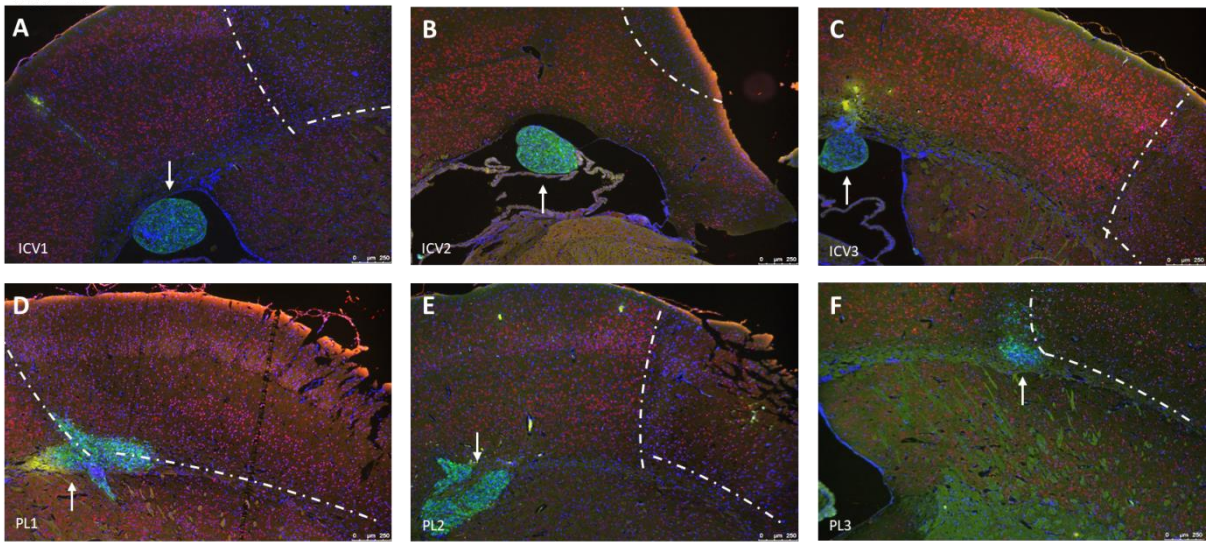

Figure 13: Positioning GFP-DPSC relative to stroke lesion. Transplantations of GFP-transduced DPSC in permanent dMCAO mice sacrificed one day after DPSC transplantation. **(A-C)** After ICV injection GFP-transduced DPSC could be detected in the lateral ventricles of the mice. **(D-E)** PL injection GFP-DPSC also resulted in traceable cells close to the lesion. The presence of NeuN expression is presented in red, GFP positive cells are visible in green and nuclei staining with DAPI indicated in blue. The ischemic border zone is marked with a dashed line and the presence of green fluorescent cells with an arrow. (N=3, magnification 5x, and scale bar = 200 µm)

To evaluate the survival time of transplanted DPSC in the lateral ventricles and the PL area, an experiment on 12 dMCAO mice, which were sacrificed one day and seven days after stem cell transplantation, was performed. Immunohistochemical analysis of NeuN was performed on the samples of mice sacrificed seven days after transplantation and compared with the samples of previously described analysis (*figure 13*), of mice sacrificed one day after transplantation.

Green fluorescent cells are detected one day after transplantation with both administration methods (*figure 14 A-F*). This occurrence is visible in the mice sacrificed seven days post-transplantation. After seven days, no GFP expressing DPSC are detected in the lateral ventricles with the ICV injection method (*figure 14 G-I*). However, after seven days, a green fluorescent signal is visible in the PL injected mice (figure 14 J-L). The dashed circle indicates these green fluorescent cells. Besides, on figure 14 J and L, another green, but less bright, fluorescent signal is detected (indicated by the arrow).

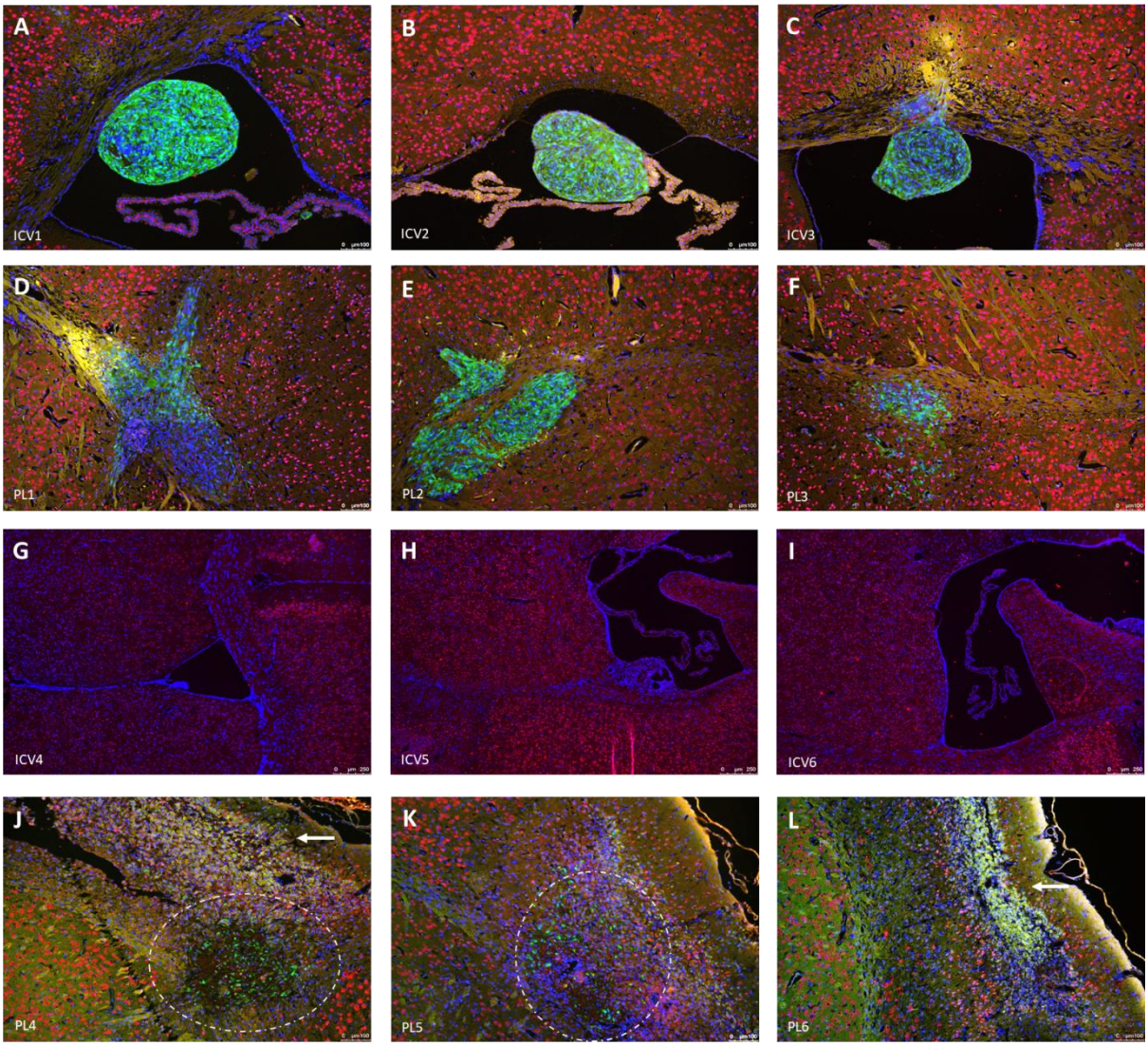

Figure 14: Survival of GFP-DPSC in stroke lesion. Transplantations of GFP-transduced DPSC in permanent dMCA mice sacrificed one and seven days after DPSC transplantation. **(A-C)** ICV injected and **(D-F)** PL injected dMCAO mice with GFP transduced DPSC, one day after transplantation show GFP expressing cells. **(G-I)** ICV injected mice seven days after transplantation reveal no GFP expressing cells. **(J-L)** Analysis of PL injected mice seven days after transplantation reveal green fluorescent cells (indicated with the dashed circle) and an additional bright green fluorescent signal (indicated with an arrow). (N=6, magnification 10X applied for pictures (A-F) and (J-K) and magnification 5x for (G-I), Scale bar A-F and J-L = 100 µm and G-I = 250 µm)

3.5.3. Validation of stem cell identity with immunohistochemical analysis of vimentin

Immunohistochemical analysis of vimentin was performed to validate the origin of previously detected GFP positive cells. This test was necessary to reinsure true GFP-DPSC were detected. Vimentin is a marker mainly expressed in mesenchymal cells. For this experiment, an antibody with no cross-reactivity for mice was used. Therefore, the cells detected by this analysis cannot have a mice origin and must be the injected human DPSC. Representative pictures of the experiment were shown. The previously detected green-fluorescent cells, in the PL and ICV injected mice, all express vimentin (*figure 15*). This confirms the results of the previous experiment. On the position where an additional fluorescent signal is detected (arrows *figure 14 J and L*) no vimentin expression is

seen. However, on the PL injected tissue sample seven days after transplantation (*figure 14 L*) were no green fluorescent cells are detected, a small area of vimentin expressing cells is still present (picture not shown).

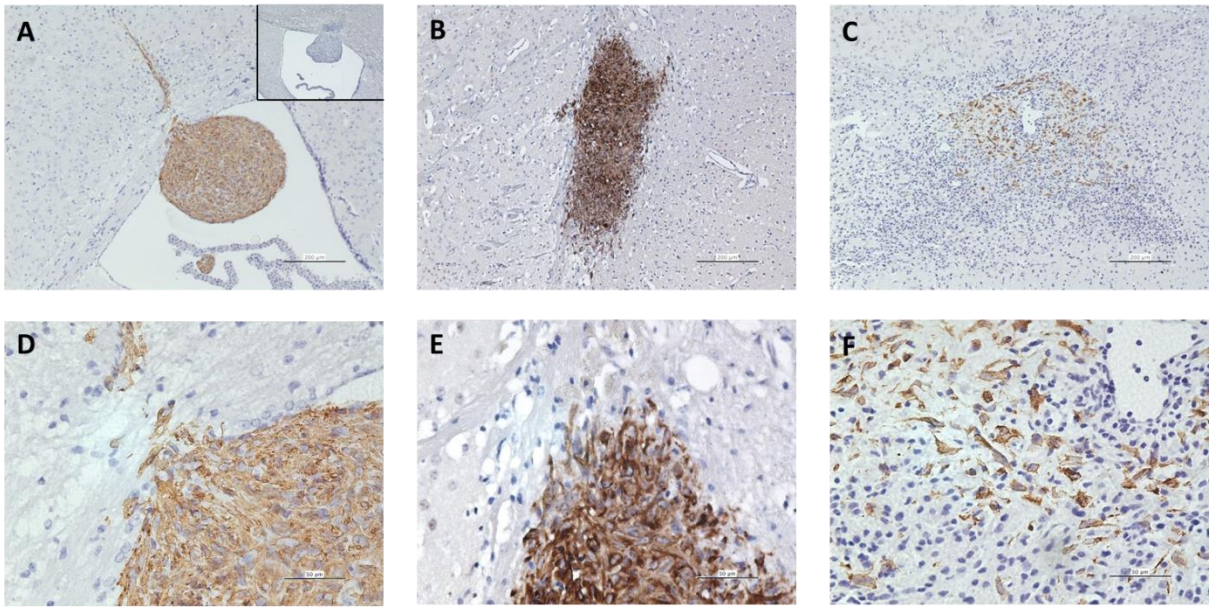

Figure 15: Validation of DPSC transplantation by expression of vimentin. Vimentin expressing cells indicated by DAB staining in mice with GFP-DPSC transplantations. Picture **A** and **D** show vimentin expression in ICV injected mice after day one. Picture **B** and **E** indicate the vimentin-positive cells after one day post PL transplantation and picture **C** and **E** show the positive cells seven days after PL transplantation. (magnification A-C = 10x and D-F= 40x, Scale bar A-C=200µm and D-F=50µm)

3.5.4. Expression of GFAP and IBA-1 in GFP-DPSC transplanted stroke brains

Expression of GFAP in ischemic brain injury is associated with the activation of astrocytes. Ionized calcium-binding adapter molecule-1 (IBA-1) expression is linked with the presence of activated microglial cells and infiltrating macrophages. During this experiment, the localization of IBA-1 and GFAP expression in the surrounding zone of the transplanted GFP-DPSC was analyzed in mice sacrificed one day and seven days after GFP-DPSC transplantation (*figure 16*). Both GFAP and IBA-1 positive cells (red) are present one day and seven days after stem cell transplantation. The amount of IBA-1 positive cells is strongly upregulated after seven days. GFAP expression seven days post injection is in particular situated in the ischemic border zone as indicated by the arrows. Lower expression levels of IBA-1 and GFAP are detected in the area were most green fluorescent signal is seen. However, in the area where a green fluorescent signal could be seen, yet no vimentin expression is detected (figure 14 J and L), a high IBA-1 expression is present.

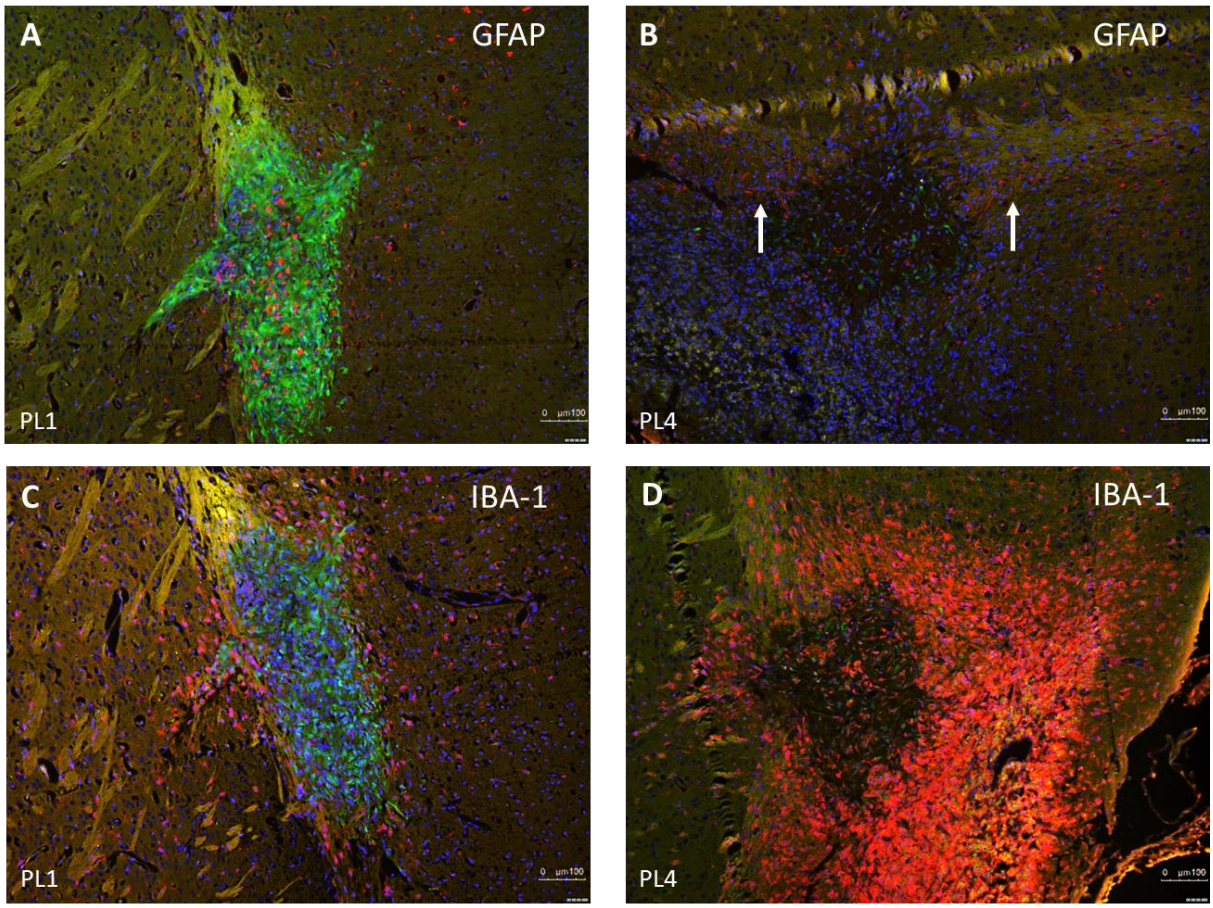

Figure 16: expression of GFAP and IBA-1 in DPSC injected stroke brains. Expression of GFAP and IBA-1 in dMCAO mice with GFP-transduced DPSC transplantations. **(A)** expression of GFAP in stroke brain one day after DPSC injection. **(B)** A thin border of GFAP positive cells was seen at the ischemic border in stroke brain seven days after DPSC injection. **(C)** IBA-1 positive cells surrounding the GFP-DPSC in stroke brain one day after DPSC injection **(D)** show distinguishing expression of IBA-1 but not in the area were most green fluorescent cells are detected, seen in stroke brain seven days after DPSC injection. IBA-1 and GFAP expression are indicated in red, GFP positive cells in green, and the nuclei are stained with DAPI in blue. (Magnification 10x and Scale bar=100 µm)

3.6. Characterization of endogenous NSC

To evaluate the presence of endogenous activated NSC, by stroke, in the SVZ of the lateral ventricles; the expression of DCX and PSA-NCAM was analyzed. This evaluation is performed with immunohistochemistry on *ex vivo* samples of mice sacrificed eight days post-stroke. After analysis, DCX-positive cells are detected in de SVZ of the lateral ventricles (Figure 17A) and the granular zone of the dentate gyrus (indicated by the arrow) (Figure 17B). More directed towards the cerebral cortex in the area where the lesion is situated DCX positive cells are found. Subsequently, the expression of PSA-NCAM positive cells is seen in the SVZ of the lateral ventricles (Figure 17 D, E, F).

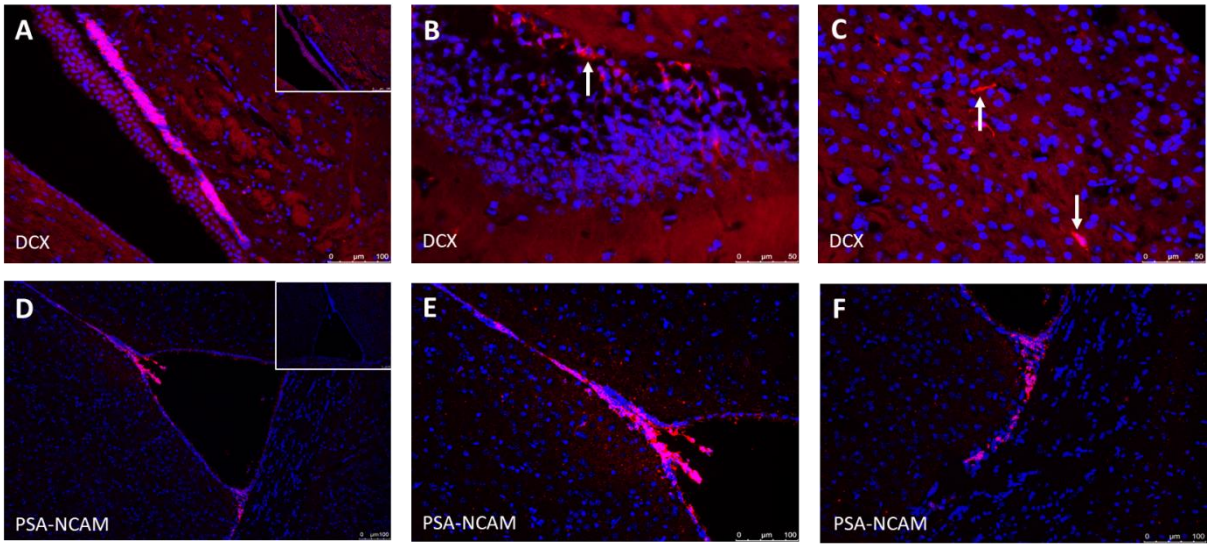

Figure 17: Expression of DCX and PSA-NCAM in stroke brains. The expression of DCX and PSA-NCAM in the SVZ of dMCAO mice eight days post stroke was evaluated. **(A)** Shows the DCX positive cells in SVZ at magnification 20x. **(B)** Indicates the presence of DCX expressing cells in the dentate gyrus (40x) and **(C)** in proximity of the ischemic lesion (40x). **(D-F)** Expression of PSA-NCAM can be detected in the SVZ of the lateral ventricle in stroke mice at magnification 10x (D) and 20x (E and F). (Scale bar A and D-F=100 µm, and B and C=50 µm)

4. Discussion

It is a widely accepted idea that the transplantation of stem cells is an attractive method to cure diseases such as ischemic stroke. Certainly, for long-term approaches where current treatment procedures tend to fail, stem cells can provide alternatives to heal or regenerate the injured tissue. In the last decennia, the potential of mesenchymal stem cells to improve the recovery after ischemic stroke has been revealed. Several studies with MSC show promising results, and the MSC was indicated to possess beneficial neuroregenerative effects mainly devoted to its secretion of paracrine factors (81). As a result, the idea to combine the secretory abilities of MSC with the overexpression of a neuroregenerative growth factor emerged (83). In this study, the goal was to investigate and compare the neuroregenerative effects of IGF-2 and two engineered variants Des[1-6] and Arg6 IGF-2. To select the most potent variant to generate a lentiviral DNA construct required for the development of an IGF-2-overexpressing DPSC cell line. Further, it was validated if DPSC are ideal stem cells for this cell therapy in ischemic stroke.

DPSC therapies can be beneficial for stroke, mainly due to their secretory character (81). Our preliminary data showed that IGF-2 is present in high quantities of the DPSC secretome (data not shown). The results of this study revealed that the average IGF-2 secretion of DPSC was 175.3 pg/ml/1x10^5 cells, which was significantly higher than with HDF 117.6 pg/ml/1x10^5 cells. Additionally, the IGF-2 secretion of DPSC was also higher than that of BM-MSC 114.2 pg/ml/1x10^5 cells, which are the most extensively studied and considered as the golden standard for MSC stem cell therapies. Revealing the use of DPSC is more favorable then BM-MSC. This result confirms the use of DPSC to generate an IGF-2 overexpressing cell line.

The growth factor IGF-2 has a variety of paracrine and autocrine effects. It is of great importance during growth, cellular maturation, and cell survival (88). Data with knock-out mice revealed that IGF-2 is involved in total body growth and organ development. The IGF-2 knock-out in mice was not lethal, but the lack of IGF-2 expression resulted in smaller mice with a weight reduction of 40%. In the last decennia, the idea of IGF-2 playing a supportive role in neurogenesis became more accepted (90). In the adult brain, IGF-2 is mainly produced by the choroid plexus. This branching network of modified ependymal cells is the producer of the cerebrospinal fluid and responsible for maintaining the NSC population by the secretion of proteins such as leukemia inhibitory factor and ciliary neurotrophic factor (90, 91). Ziegler et al. discovered that IGF-2 could induce NSC expansion, and our preliminary data indicated IGF-2 can to stimulate NSC migration which are two essential processes during neurogenesis (92). IGF-2 can bind three different receptors, the IGF-1 receptor which has a high affinity for both IGF-1 and IGF-2, the IGF-2/mannose 6-phosphate receptor which is mainly considered a scavenger receptor of IGF-2, and the insulin receptor A isoform (92). The pleiotropic effects of IGFs are not only regulated by its receptor-mediated effects, but another role is also played by the IGF binding proteins. Six different IGBPs are binding to free IGFs with a high affinity. They are mainly present in areas related to the IGF receptor binding sites and therefore, the IGFBPs will compete with the IGF receptors over IGFs. In general, this IGFBP binding results in an inhibitory effect on the IGFs. Nonetheless, some IGFBPs

can enhance certain pleiotropic effects of IGFs, depending on the process, location and concentration (93). One of the IGFBPs known for its inhibitory effect on IGF-2 is IGFBP-6. It has a 50 times higher affinity for IGF-2 than IGF-1 and is mostly known for its IGF-2 directed effects, such as inhibition of migration induced by IGF-2 (84). IGFBP-6 can also alter intracellular signaling pathways and with this alter transcription on an IGF-independent way. Contradictory, IGFBP-6 alone was also described to have IGF-independent effects like a migratory effect on, for example, colon cancer cells, and an inhibitory effect on angiogenesis (84, 94, 95). To investigate the role of IGFBPs on IGF-2 Francis G.L. et al. produced in 1993 two IGF-2 analogs, Des[1-6] and Arg6 IGF-2. Both variants lack an IGFBP binding site and are therefore considered to be less prone for IGFBP inhibition. The analogs also have an increased affinity for the IGF2R, of both analogs; this increase is more prominent with the Arg6 variant (96).

In order to verify whether the use of these IGF-2 analogs could be more beneficial compared to normal IGF-2, migration of NSC was first tested. To test if the Arg6 and Des[1-6] IGF-2 analogs are equal or even better than the wild type IGF-2 transwell migration assays were performed. Both analogs were able to stimulate NSC migration. Nevertheless, our results showed that both the engineered variants could stimulate NSC migration more than IGF-2 in the adjacency of 10 and 100 ng/ml IGFBP-6. At a concentration of 100 ng/ml IGFBP-6, the Arg6 IGF-2 induced migration was even significantly less inhibited by IGFBP-6 then the migration induced by normal IGF-2. After power calculation of the performed experiment (N=5) with effect size 3,3 and power 0,80; it came to notice still one repetition of the experiment may be required to prove the significant difference in migration between the Des[1-6] analog and WT IGF-2 at a concentration of 100 ng/ml IGFBP-6. This resilience of these IGF-2 analogs against IGFBP-6 inhibition will most likely be devoted to their altered affinity for the IGFBPs. However, at a concentration of 1000 ng/ml on all the three experimental conditions, IGF-2 induced migration was inhibited. This decrease indicates IGFBP-6 can still inhibit the IGF-2 analogs, yet, this inhibition is less pronounced in the analogs at lower concentrations of IGFBP-6. The resilience of these analogs against IGFBP-6 inhibition increases their therapeutic value for neuroregenerative therapies. Because NSC migration is an essential process during neurogenesis, the administration of IGF-2 can possibly improve this natural process. However, due to their altered affinity for the endogenous present IGFBP-6, the IGF-2 variants can be even more potent and can have a stronger migratory effect *in vivo.* Therefore, use of these analogs is the preferred option over WT IGF-2 to be applied in an IGF-2 overexpressing dental pulp stem cell line.

Another potent effect of IGF-2 is its ability to induce NSC expansion. Ziegler et. al indicated IGF-2 plays a role in the expansion of NSC cultures, as well IGF-2 was identified to be a key player in proliferation induced by the cerebrospinal fluid *in vivo* (92, 97). Regarding this knowledge, it is questionable whether an increase in NSC proliferation influenced the observed IGF-2 induced migration. Therefore, the proliferative effects of IGF-2 and DPSC conditioned medium were tested under similar circumstances as the migration assays. No proliferation was observed within the experimental setting. Instead, less than 100% of the NSC could survive for longer than 24 h on the tested conditions. After 48 h, a 50% decrease in the surviving cells could be detected. With the negative control, first a small proliferating trend was seen after 24 h and later only a slow

decrease in cell survival was detected. This confirms that the NSC migration seen during the transwell migration assay was indeed true migration and not caused by an increase in cell count as a result of proliferation. Based on these findings, it cannot be concluded whether IGF-2 enables to stimulate proliferation of NSC or not, these conditions were optimized for a transwell migration assay. Therefore, they were most likely not optimal to stimulate proliferation. However, to validate the proliferative aspects of IGF-2 observed by Ziegler et al., a different set-up on growth medium should be suited to investigate the proliferative capacity of IGF-2.

The NSC used during in vitro assays were characterized utilizing immunocytochemistry. They showed expression of CD133, EGFR, DCX, and SOX2. The NSC lacked expression of PSA-NCAM, β3-tubulin, and GFAP. During the activation of the NSC from a quiescent state towards an activated and further into a migrating neuroblast, the phenotype changes. In the early stages of development, NSC express markers such as GFAP and CD133. When activated, the NSC become more proliferative and lose expression of GFAP, while gaining expression of EGFR and SOX2 (98). In later stages, when the NSC is further developed into a neuroblast, DCX, and PSA-NCAM are expressed (57). Based on the expression levels of our NSC it could be said that they are situated in a later stage of development. However, they do not show expression of PSA-NCAM, a late neuroblast marker, and lack expression of β3-tubulin, a neuronal marker (57, 99).

Another interesting aspect of IGF-2 which has been described is its pro-angiogenic character. It was revealed that IGF-2 induces migration and tube formation of human umbilical vein endothelial cells (HUVEC) cells (100, 101). Which are two clear indications that IGF-2 can enhance angiogenesis. The pro-angiogenic effects of the IGF-2 analogs Des[1-6] and Arg6 were never before tested. Our results showed that both the analogs could, as well as WT IGF-2, induced HMEC-1 migration at a concentration of 100 ng/ml IGF-2. The Des[1-6] analog as well as IGF-2 showed to induce significantly more HMEC-1 migration than α-mem at a concentration of 100 ng/ml. However, at 1 ng/ml and 10 ng/ml, the migration were almost similar to the negative control. This result suggests the migratory response of HMEC-1 towards IGF-2 will most likely start somewhere between 10 and 100 ng/ml. Because the IGF-2 analogs are able to stimulate migration of endothelial cells, which is an essential process in angiogenesis; it is to expect that the administration of the IGF-2 variants can enhance angiogenesis. This ability makes the use of IGF-2 very potent for ischemic stroke therapy. Knowing that after the ischemic conditions of a stroke the neurovasculature is gravely disturbed, the use of a pro-angiogenic growth factor can be beneficial to enhance recovery (46).

As previously described the Arg6 variant has a higher affinity for the IGF2R as WT IGF-2 and the Des[1-6] IGF-2 variant. Because so little is known about the IGF2R, the use of the Arg6 variant will be less predictable and possible less comparable to the effects of normal IGF-2. Therefore, and because previously described observations considering the pro-angiogenic and neurogenic effects of the IGF-2 variants; The Des[1-6] IGF-2 analog was decided to be the most optimal IGF-2 variant for an IGF-2-DPSC cell line.

In order to generate a Des[1-6] IGF-2 stem cell line by means of transduction, a lentiviral vector has to be made. The use of lentiviral vectors is a favorable choice to generate overexpression of transgenes in a cell line. They can introduce themselves into the genomic DNA of the host and are able to generate a stable expression of the inserted transgene. Additionally, lentiviral vectors can transduce dividing and non-dividing cells (102, 103). The expression of the transgene cannot be silenced after lentiviral transduction, a phenomenon observed in most retroviruses (104). Currently, second and third generation lentiviral systems are the preferred option. Existing out of several individual components these systems are much safer than their predecessor because they are unable to self-replicate. 3rd generation lentiviral systems exist out of a transfer plasmid containing the transgene, an envelope plasmid, and two packaging plasmids (103, 105). A transfer plasmid containing Des[1-6] IGF-2 and a plasmid containing wild type IGF-2 were produced. However, after validation with restriction digestion, it came to notice that these plasmids possessed unwanted DNA fragments. A cause could be the occurrence of star activity (106). During this phenomenon, some restriction enzymes have an altered activity under non-standard conditions and are therefore able to cut non-specific targets. However, to compensate for star activity, another restriction with different enzymes of this plasmid was performed (data not showed). Another possibility could be the occurrence of partial restriction digestion. This phenomenon could be devoted to high salt concentrations resulting for example of DNA purification and can result in more than expected fragments (107). An alternative explanation could be the occurrence of an external DNA fragment incorporated in the plasmid DNA. This may originate from the original plasmid or the inserted fragments. To confirm the origin of this additional fragment after gel electrophoreses; a Sanger sequencing of the plasmid can be performed. If the source of the unwanted fragment is determined corrections can be made where necessary, and the sub-cloning of the required plasmid can be repeated.

Further, it has to be determined if DPSC can be correctly transplanted in a stroke brain and whether they are able to survive after transplantation. To study the effects of DPSC transplantations on ischemic stroke *in vivo;* a mice model for stroke is required. A commonly adopted and well-described approach to simulate an ischemic stroke in an animal model, is the occlusion of the middle cerebral artery (MCAO). The MCA is the most frequent occluded artery during ischemic stroke in humans. The use of this model is therefore considered to be more representative towards future clinical studies. The MCA model can be permanent or transient. Depending on the research question different manners to induce the ischemia can be mediated, for example, the use of an intra-arterial suture is commonly applied (108). In this study, the mouse model with permanent occlusion of the distal middle cerebral artery (dMCAO) has been used. It generates cortical ischemia mainly in the somatosensory cortex. Further, this model generates highly reproducible lesions and has low mortality rates which makes it very suited to investigate a neuroregenerative therapy on stroke (109-111). Within our research group expertise regarding the use of the permanent dMCAO model is well established. With this knowledge, replicable lesions can be produced. To validate the presence of a lesion and the consistency of the generated lesion volume a TTC assay was performed. The molecule 2,3,5-triphenyl-tetrazolium chloride is reduced during the redox reaction with succinate dehydrogenase into the red 1,3,5-triphenylformazan (112). However, the reaction can only occur in metabolic active and thus viable cells. This permits

to make a distinction between the lesion and healthy tissue. (89). It generated an average lesion size of the ipsilesional hemisphere of 14.79% with a SEM of 3.52%. The variability in the lesion volume will most likely originate from biological and methodological variance (113). Due to the processing method after isolation of the brains, often an over or under-estimation of the hemisphere surfaces was made. Therefore, the most variance was likely devoted to alterations during area % measurement of each brain slide.

The process of neurogenesis is known to be upregulated after stroke. The activated NSC tend to start to migration from the SVZ via the corpus callosum towards the stroke lesion (61). Our results confirmed that this process also occurred in the dMCAO model in mice. Both DCX and PSA-NCAM markers for migrating NSC were detected in the SVZ (61, 114). DCX expression was also present in some cells around the stroke lesion, indicating the presence of migrated NSC.

Furthermore, immunohistochemical analyses of the dMCAO stroke lesion was performed. NeuN can be detected in post-mitotic neurons and is present in the nuclei of all mature neurons. The NeuN epitope is a phosphorylated protein which originates from the Rbfox3 gene located on chromosome 11. NeuN stainings are useful to visualize the stroke lesion since the immunoreactivity greatly decreases in areas with dead neurons. In MCAO rats, a decrease of 62% of NeuN positive neurons was seen in the ischemic core (115). Although we did not quantify the NeuN positive neurons, a visible decrease in NeuN-positive cells was observed in the dMCAO model.

Concerning the stem cell transplantations in the dMCAO model, we can conclude that the stem cells can be transplanted with moderate accuracy in the brain via stereotactical injection. Our results show that both ICV and PL transplantation were successful. With the perilesional administration method, GFP-DPSC were able to survive at least for seven days after the transplantation, while the GFP-DPSC in the ventricles could not be detected anymore. Based on these results, the use of a PL administration strategy was concluded the favorable injection method over ICV injections. The presence of the transplanted DPSC was validated with immunodetection of vimentin. Vimentin is a marker expressed by mesenchymal cells. During this study, an antibody with no-cross reactivity for the species mouse was used. As a result, it can be confirmed that the detected cells are indeed the transplanted human DPSC. Only a few studies with DPSC transplantations in stroke mice were already performed (72, 116). Leong et al. showed that the transplantation of DPSC in the cortex and striatum can improve the recovery after stroke. However, only a small fraction of the transplanted cells could be detected four weeks after transplantation. This indicated that the recovery was most likely not the result of tissue replacement but rather a consequence of the paracrine secretions released by the DPSC (72). Therefore, the survival of DPSC for at least seven days, which was detected during our study, is favorable to mediate a long-term therapeutic effect. Due to this long survival time, a continuous release of IGF-2 and other paracrine factors can take place. This release is beneficial for a neuroregenerative therapy. IGF-2 decays relatively fast. Free IGF-2 has a half-life of 10-12 min *in vivo*. When bound to IGFBPs, the half-life of IGF-2 is prolonged up to 12-15 hours (117). The fast IGF-2 decay will not influence this method, and a continuous stimulus to enhance neurogenesis and angiogenesis can be mediated. This indicates the benefit of a stem cell therapy compared to a single administration method where only one or several doses of IGF-2 can be administered, and the potent effects stop after IGF-2 decay.

In order to investigate whether stem cell transplantation alters the response in the brain after dMCAO, immunohistochemical stainings have been optimized for future experiments. After an infarction, the lesion area becomes populated with different cell types. Depending on the moment in time astroglia, activated microglial cells, macrophages are present in the ischemic area. In order to characterize this population, an immunohistochemical analysis of IBA-1 and GFAP was performed. IBA-1 is a marker expressed by activated microglia and macrophages, and GFAP is a protein mainly seen in activated astrocytes (118). Immunohistochemical analysis showed some IBA-1 expressing cells around the transplanted DPSC one day after transplantation, but an enormous amount of IBA-1 positive cells could be observed seven days after transplantation. Within the first 12 h post-stroke microglia tend to start upregulating expression of IBA-1. However, peripheral macrophages begin to infiltrate the brain only several days after a stroke. This suggests the IBA-1 expression one day after transplantation was most certainly generated by activated microglia, but the enormous increase in IBA-1 signal seven days post-transplantation could be devoted to a combination of recruited microglia and infiltrated macrophages (119). Additionally, a lot of IBA-1 positive cells were seen in the ischemic area were a green fluorescent signal without confirmation by vimentin expression was seen. This indicated that the additional fluorescent signal was not caused by the GFP-DPSC. By a study from Li et al., the auto-fluorescent character of macrophages at wavelength 488 nm was described. It was mentioned auto-fluorescence was mainly present in larger granular macrophages (120, 121). Based on these assumptions, it could be suggested that the additional fluorescent signal could be originated from infiltrated macrophages. GFAP staining revealed that activated astrocytes were present one day after transplantation. Seven days after transplantation a barrier of astrocytes could be detected surrounding the ischemic border. Both activated microglia and activated astrocytes are involved in the glial scar formation after ischemic stroke. During this process, the reactive astrocytes tend to surround and seal the lesion site (122, 123). This phenomenon was also clearly observed during our study. The occurrence of this glial scar is beneficial to reduce lesion size expansion and stimulate revascularization. However, for long-term restoration after injury, scar formation has some adverse effects. This barrier of activated astrocytes impedes axonal regeneration and cell migration, which are crucial processes during neuroregeneration (123). It could, therefore, occur that the glial scar formation will inhibit the IGF-2 induced migration of NSC and endothelial cells *in vivo*. However, the DPSC are transplanted at the outer rim of the lesion border and were only surrounded by a small fraction of the glial cells suggesting the occurrence of a glial scar will not limit the secretion of DPSC. Further, it remains unknown if the endogenous NSC and endothelial cells can still migrate to the outer rim of the glial scar and whether they can still repair and reinforce the damaged tissue surrounding the lesion area.

To further examine the effects of IGF-2 overexpressing DPSC, a stem cell line has to be generated. If Des[1-6] IGF-2 can be successfully expressed by DPSC, the first step will be to analyze the expression levels of Des[1-6] IGF-2. Next, the migratory effects of NSC and HMEC-1 towards Des[1-6] IGF-2-DPSC CM have to be validated, and the cell counts required to mediate a response have to be determined. Further, the effects of these Des[1-6] IGF-2-DPSC will be investigated *in*

vivo. Based on our observations, we expect that Des[1-6] IGF-2 will be less inhibited by the IGFBPs *in vivo.* Because of this, we expect Des[1-6] IGF-2 to have a potent effect on NSC migration, which will result in more new, mature, and fully integrated neurons in the neuronal network. Besides, we expect to increase migration of endothelial cells and therefore enhance angiogenesis. This can mediate restoration of the blood supply in the affected area. Furthermore, the process of angiogenesis is tightly coupled with neurogenesis (46). The enhancement of angiogenesis can, therefore, even further improve the formation of new neurons. However, it remains questionable if these effects can indeed be mediated *in vivo.* After our *in vitro* results, it became clear 1 ng/ml IGF-2 was sufficient to induce an effect on NSC migration. However, for HMEC-1 migration a concentration of 100 ng/ml was required, suggesting high levels of Des[1-6] IGF-2 are required to induce angiogenesis. The success of this therapy will depend on the secretion levels of the transduced DPSC, the endogenous reaction on Des[1-6] IGF-2, and whether processes such as glial scar formation will not inhibit the induced effects.

5. Conclusion

Ischemic stroke is the second most leading cause of death worldwide and is responsible for 10-15% of the worldwide mortality. Despite extensive research, there is still a need for effective long-term treatments. In this study, we aimed to investigate and compare the neuroregenerative effects of IGF-2, and the IGF-2 analogs, Des[1-6] and Arg6. With as goal to select the variant with the most therapeutic potential to be used in a IGF-2 overexpressing DPSC cell-line. Further, we investigated if DPSC can be used for an ischemic stroke therapy.

To identify the potency of DPSC to be utilized for an IGF-2-enhanced stem cell line. The IGF-2 expression levels were analyzed. DPSC appeared to be the preferred option over BM-MSC. Further, DPSC could be successfully transplanted in the stroke brain and were able to survive for a minimum of seven days. Therefore, DPSC are able to generate a long-term therapeutic effect and are able to secrete IGF-2, and other paracrine factors for at least seven days.

Further, during this study, the potent effects of the two engineered IGF-2 variants, Des[1-6] and Arg6, were investigated. It was concluded that both variants were more potent to generate NSC migration when inhibited by IGFBP-6 then WT IGF-2. Additionally, the variants were able to stimulate HMEC-1 migration. This suggests that the IGF-2 analogs can be even more beneficial then WT IGF-2 to induce neurogenesis and angiogenesis *in vivo*.

The Des[1-6] IGF-2 analog was chosen to generate an IGF-2-DPSC cell line. A first attempt to generate a Des[1-6] IGF-2 and WT IGF-2 containing the transfer plasmid was performed. However, due to failing results further troubleshooting may be required to generate this cell line.

During future experiments, the migratory effects towards CM Des[1-6] IGF-2-DPSC first has to be validated *in vitro*. Next, *in vivo* experiments in the dMCAO mice model will be required to confirm the neuroregenerative effects of this stem cell therapy.

In conclusion, the IGF-2 variants Des[1-6] IGF-2 and Arg6 IGF-2 are able to enhance NSC migration and HMEC-1 migration *in vitro* and are less prone then WT IGF-2 for IGFBP-6 inhibition when inducing NSC migration. These results indicate the therapeutic potential of these analogs to enhance angiogenesis and neurogenesis in the stroke brain. However, it remains uncertain whether these effects can be mediated by Des[1-6] IGF-2 overexpressing DPSC. Further research in rodent models of stroke is therefore required to validate the effects of Des[1-6] IGF-2 overexpressing DPSC. If this therapy is effective, further investigations may be required which could lead to a new long-term neuroregenerative therapy for ischemic stroke.

6. References

1. Go AS, Mozaffarian D, Roger VL, Benjamin EJ, Berry JD, Blaha MJ, et al. Heart disease and stroke statistics—2014 update: a report from the American Heart Association. Circulation. 2013:01. cir. 0000441139.02102. 80.
2. Feigin VL, Norrving B, Mensah GA. Global Burden of Stroke. Circulation research. 2017;120(3):439-48.
3. Zhang C, Wang Y, Zhao X, Liu L, Wang C, Pu Y, et al. Prediction of Recurrent Stroke or Transient Ischemic Attack After Noncardiogenic Posterior Circulation Ischemic Stroke. Stroke. 2017;48(7):1835-41.
4. Khoshnam SE, Winlow W, Farbood Y, Moghaddam HF, Farzaneh M. Emerging Roles of microRNAs in Ischemic Stroke: As Possible Therapeutic Agents. Journal of Stroke. 2017;19(2):166-87.
5. Organization WH. MONICA Project (monitoring trends and determinants in cardiovascular disease): a major international collaboration. WHO MONICA Project Principal Investigators. 1988.
6. Pelisek J, Eckstein HH, Zernecke A. Pathophysiological mechanisms of carotid plaque vulnerability: impact on ischemic stroke. Archivum immunologiae et therapiae experimentalis. 2012;60(6):431-42.
7. Amarenco P, Bogousslavsky J, Caplan LR, Donnan GA, Wolf ME, Hennerici MG. The ASCOD phenotyping of ischemic stroke (Updated ASCO Phenotyping). Cerebrovascular diseases (Basel, Switzerland). 2013;36(1):1-5.
8. Jaracz K, Grabowska-Fudala B, Gorna K, Kozubski W. Consequences of stroke in the light of objective and subjective indices: a review of recent literature. Neurologia i neurochirurgia polska. 2014;48(4):280-6.
9. Jolivel V, Bicker F, Biname F, Ploen R, Keller S, Gollan R, et al. Perivascular microglia promote blood vessel disintegration in the ischemic penumbra. Acta neuropathologica. 2015;129(2):279-95.
10. El-Koussy M, Schroth G, Brekenfeld C, Arnold M. Imaging of acute ischemic stroke. European neurology. 2014;72(5-6):309-16.
11. Hu Q, Manaenko A, Bian H, Guo Z, Huang J-L, Guo Z-N, et al. Hyperbaric Oxygen Reduces Infarction Volume and Hemorrhagic Transformation Through ATP/NAD(+)/Sirt1 Pathway in Hyperglycemic Middle Cerebral Artery Occlusion Rats. Stroke. 2017;48(6):1655-64.
12. Pignataro G, Sirabella R, Anzilotti S, Di Renzo G, Annunziato L. Does Na(+)/Ca(2)(+) exchanger, NCX, represent a new druggable target in stroke intervention? Translational stroke research. 2014;5(1):145-55.
13. Murphy TH, Li P, Betts K, Liu R. Two-photon imaging of stroke onset in vivo reveals that NMDA-receptor independent ischemic depolarization is the major cause of rapid reversible damage to dendrites and spines. The Journal of neuroscience : the official journal of the Society for Neuroscience. 2008;28(7):1756-72.
14. Sorby-Adams AJ, Marcoionni AM, Dempsey ER, Woenig JA, Turner RJ. The Role of Neurogenic Inflammation in Blood-Brain Barrier Disruption and Development of Cerebral Oedema Following Acute Central Nervous System (CNS) Injury. International journal of molecular sciences. 2017;18(8):1788.
15. Zhu S, Tang S, Su F. Dioscin inhibits ischemic strokeinduced inflammation through inhibition of the TLR4/MyD88/NFkappaB signaling pathway in a rat model. Molecular medicine reports. 2018;17(1):660-6.
16. L L, X W, Z Y. Ischemia-reperfusion Injury in the Brain: Mechanisms and Potential Therapeutic Strategies. Biochemistry & pharmacology : open access. 2016;5(4):213.
17. Saver JL, Goyal M, van der Lugt A, Menon BK, Majoie CB, Dippel DW, et al. Time to Treatment With Endovascular Thrombectomy and Outcomes From Ischemic Stroke: A Meta-analysis. Jama. 2016;316(12):1279-88.
18. Micieli G, Marcheselli S, Tosi PA. Safety and efficacy of alteplase in the treatment of acute ischemic stroke. Vascular health and risk management. 2009;5(1):397-409.
19. Powers WJ, Derdeyn CP, Biller J, Coffey CS, Hoh BL, Jauch EC, et al. 2015 American Heart Association/American Stroke Association Focused Update of the 2013 Guidelines for the Early Management of Patients With Acute Ischemic Stroke Regarding Endovascular Treatment: A Guideline for Healthcare Professionals From the American Heart Association/American Stroke Association. Stroke. 2015;46(10):3020-35.
20. Goyal M, Menon BK, Van Zwam WH, Dippel DW, Mitchell PJ, Demchuk AM, et al. Endovascular thrombectomy after large-vessel ischaemic stroke: a meta-analysis of individual patient data from five randomised trials. The Lancet. 2016;387(10029):1723-31.
21. Fischer S, Weber W. Vascular medicine and thrombectomy in stroke. Therapeutic advances in neurological disorders. 2017;11:1756285617742082-.
22. Lapergue B, Blanc R, Guedin P, Decroix JP, Labreuche J, Preda C, et al. A Direct Aspiration, First Pass Technique (ADAPT) versus Stent Retrievers for Acute Stroke Therapy: An Observational Comparative Study. AJNR American journal of neuroradiology. 2016;37(10):1860-5.
23. Merlino G, Sponza M, Petralia B, Vit A, Gavrilovic V, Pellegrin A, et al. Short and long-term outcomes after combined intravenous thrombolysis and mechanical thrombectomy versus direct mechanical thrombectomy: a prospective single-center study. Journal of thrombosis and thrombolysis. 2017;44(2):203-9.
24. Powers WJ, Rabinstein AA, Ackerson T, Adeoye OM, Bambakidis NC, Becker K, et al. 2018 guidelines for the early management of patients with acute ischemic stroke: a guideline for healthcare

professionals from the American Heart Association/American Stroke Association. Stroke. 2018;49(3):e46-e99.
25. Mistry EA, Mistry AM, Nakawah MO, Chitale RV, James RF, Volpi JJ, et al. Mechanical Thrombectomy Outcomes With and Without Intravenous Thrombolysis in Stroke Patients: A Meta-Analysis. Stroke. 2017;48(9):2450-6.
26. Krawczyk M, Szczerbik E, Syczewska M. The comparison of two physiotherapeutic approaches for gait improvement in sub-acute stroke patients. Acta of bioengineering and biomechanics. 2014;16(1):11-8.
27. Dobkin BH. Strategies for stroke rehabilitation. The Lancet Neurology. 2004;3(9):528-36.
28. Sundseth A, Thommessen B, Ronning OM. Outcome after mobilization within 24 hours of acute stroke: a randomized controlled trial. Stroke. 2012;43(9):2389-94.
29. Veltkamp R, Gill D. Clinical Trials of Immunomodulation in Ischemic Stroke. Neurotherapeutics : the journal of the American Society for Experimental NeuroTherapeutics. 2016;13(4):791-800.
30. Santos Samary C, Pelosi P, Leme Silva P, Rieken Macedo Rocco P. Immunomodulation after ischemic stroke: potential mechanisms and implications for therapy. Critical care (London, England). 2016;20(1):391-.
31. Ao LY, Yan YY, Zhou L, Li CY, Li WT, Fang WR, et al. Immune Cells After Ischemic Stroke Onset: Roles, Migration, and Target Intervention. Journal of molecular neuroscience : MN. 2018;66(3):342-55.
32. Clausen BH, Lambertsen KL, Babcock AA, Holm TH, Dagnaes-Hansen F, Finsen B. Interleukin-1beta and tumor necrosis factor-alpha are expressed by different subsets of microglia and macrophages after ischemic stroke in mice. Journal of neuroinflammation. 2008;5:46-.
33. Gliem M, Mausberg AK, Lee JI, Simiantonakis I, van Rooijen N, Hartung HP, et al. Macrophages prevent hemorrhagic infarct transformation in murine stroke models. Ann Neurol. 2012;71(6):743-52.
34. Gu L, Jian Z, Stary C, Xiong X. T Cells and Cerebral Ischemic Stroke. Neurochemical research. 2015;40(9):1786-91.
35. Liesz A, Hu X, Kleinschnitz C, Offner H. Functional role of regulatory lymphocytes in stroke: facts and controversies. Stroke. 2015;46(5):1422-30.
36. Emsley HC, Smith CJ, Georgiou RF, Vail A, Hopkins SJ, Rothwell NJ, et al. A randomised phase II study of interleukin-1 receptor antagonist in acute stroke patients. Journal of neurology, neurosurgery, and psychiatry. 2005;76(10):1366-72.
37. Fu Y, Zhang N, Ren L, Yan Y, Sun N, Li YJ, et al. Impact of an immune modulator fingolimod on acute ischemic stroke. Proceedings of the National Academy of Sciences of the United States of America. 2014;111(51):18315-20.
38. Wang Y, Liu G, Hong D, Chen F, Ji X, Cao G. White matter injury in ischemic stroke. Progress in neurobiology. 2016;141:45-60.
39. Joseph MJ, Caliaperumal J, Schlichter LC. After Intracerebral Hemorrhage, Oligodendrocyte Precursors Proliferate and Differentiate Inside White-Matter Tracts in the Rat Striatum. Translational stroke research. 2016;7(3):192-208.
40. Wang C, Zhang Y, Ding J, Zhao Z, Qian C, Luan Y, et al. Nicotinamide Administration Improves Remyelination after Stroke. Neural plasticity. 2017;2017:7019803-.
41. Zhang RL, Chopp M, Roberts C, Wei M, Wang X, Liu X, et al. Sildenafil enhances neurogenesis and oligodendrogenesis in ischemic brain of middle-aged mouse. PloS one. 2012;7(10):e48141-e.
42. Jiang Q, Zhang ZG, Ding GL, Silver B, Zhang L, Meng H, et al. MRI detects white matter reorganization after neural progenitor cell treatment of stroke. NeuroImage. 2006;32(3):1080-9.
43. Venkat P, Chopp M, Chen J. New insights into coupling and uncoupling of cerebral blood flow and metabolism in the brain. Croatian medical journal. 2016;57(3):223-8.
44. Shabir O, Berwick J, Francis SE. Neurovascular dysfunction in vascular dementia, Alzheimer's and atherosclerosis. BMC neuroscience. 2018;19(1):62-.
45. Sun F-L, Wang W, Cheng H, Wang Y, Li L, Xue J-L, et al. Morroniside improves microvascular functional integrity of the neurovascular unit after cerebral ischemia. PloS one. 2014;9(6):e101194-e.
46. Krupinski J, Kaluza J, Kumar P, Kumar S, Wang JM. Role of angiogenesis in patients with cerebral ischemic stroke. Stroke. 1994;25(9):1794-8.
47. Delle Monache S, Alessandro R, Iorio R, Gualtieri G, Colonna R. Extremely low frequency electromagnetic fields (ELF-EMFs) induce in vitro angiogenesis process in human endothelial cells. Bioelectromagnetics. 2008;29(8):640-8.
48. Cichon N, Bijak M, Miller E, Saluk J. Extremely low frequency electromagnetic field (ELF-EMF) reduces oxidative stress and improves functional and psychological status in ischemic stroke patients. Bioelectromagnetics. 2017;38(5):386-96.
49. Urnukhsaikhan E, Mishig-Ochir T, Kim SC, Park JK, Seo YK. Neuroprotective Effect of Low Frequency-Pulsed Electromagnetic Fields in Ischemic Stroke. Applied biochemistry and biotechnology. 2017;181(4):1360-71.
50. Marushima A, Nieminen M, Kremenetskaia I, Gianni-Barrera R, Woitzik J, Degenfeld GV, et al. Balanced single-vector co-delivery of VEGF/PDGF-BB improves functional collateralization in chronic cerebral ischemia. Journal of cerebral blood flow and metabolism : official journal of the International Society of Cerebral Blood Flow and Metabolism. 2019:271678x18818298.
51. Ruan L, Wang B, ZhuGe Q, Jin K. Coupling of neurogenesis and angiogenesis after ischemic stroke. Brain research. 2015;1623:166-73.
52. Ohab JJ, Fleming S, Blesch A, Carmichael ST. A neurovascular niche for neurogenesis after stroke. The Journal of neuroscience : the official journal of the Society for Neuroscience. 2006;26(50):13007-16.
53. Lepousez G, Nissant A, Lledo PM. Adult neurogenesis and the future of the rejuvenating brain circuits. Neuron. 2015;86(2):387-401.

54. Jia S, Liu Y, Shi Y, Ma Y, Hu Y, Wang M, et al. Elevation of Brain Magnesium Potentiates Neural Stem Cell Proliferation in the Hippocampus of Young and Aged Mice. Journal of cellular physiology. 2016;231(9):1903-12.
55. Braun SM, Jessberger S. Adult neurogenesis: mechanisms and functional significance. Development (Cambridge, England). 2014;141(10):1983-6.
56. Zelentsova K, Talmi Z, Abboud-Jarrous G, Sapir T, Capucha T, Nassar M, et al. Protein S Regulates Neural Stem Cell Quiescence and Neurogenesis. Stem cells (Dayton, Ohio). 2017;35(3):679-93.
57. Dulken BW, Leeman DS, Boutet SC, Hebestreit K, Brunet A. Single-Cell Transcriptomic Analysis Defines Heterogeneity and Transcriptional Dynamics in the Adult Neural Stem Cell Lineage. Cell reports. 2017;18(3):777-90.
58. Llorens-Bobadilla E, Zhao S, Baser A, Saiz-Castro G, Zwadlo K, Martin-Villalba A. Single-Cell Transcriptomics Reveals a Population of Dormant Neural Stem Cells that Become Activated upon Brain Injury. Cell stem cell. 2015;17(3):329-40.
59. Kempermann G, Song H, Gage FH. Neurogenesis in the Adult Hippocampus. Cold Spring Harbor perspectives in biology. 2015;7(9):a018812-a.
60. Sun W, Winseck A, Vinsant S, Park OH, Kim H, Oppenheim RW. Programmed cell death of adult-generated hippocampal neurons is mediated by the proapoptotic gene Bax. The Journal of neuroscience : the official journal of the Society for Neuroscience. 2004;24(49):11205-13.
61. Tang H, Wang Y, Xie L, Mao X, Won SJ, Galvan V, et al. Effect of neural precursor proliferation level on neurogenesis in rat brain during aging and after focal ischemia. Neurobiology of aging. 2009;30(2):299-308.
62. Boareto M, Iber D, Taylor V. Differential interactions between Notch and ID factors control neurogenesis by modulating Hes factor autoregulation. Development (Cambridge, England). 2017;144(19):3465-74.
63. Heldmann U, Thored P, Claasen JH, Arvidsson A, Kokaia Z, Lindvall O. TNF-alpha antibody infusion impairs survival of stroke-generated neuroblasts in adult rat brain. Experimental neurology. 2005;196(1):204-8.
64. Jin Y, Barnett A, Zhang Y, Yu X, Luo Y. Poststroke Sonic Hedgehog Agonist Treatment Improves Functional Recovery by Enhancing Neurogenesis and Angiogenesis. Stroke. 2017;48(6):1636-45.
65. Zhang RL, Zhang ZG, Lu M, Wang Y, Yang JJ, Chopp M. Reduction of the cell cycle length by decreasing G1 phase and cell cycle reentry expand neuronal progenitor cells in the subventricular zone of adult rat after stroke. Journal of cerebral blood flow and metabolism : official journal of the International Society of Cerebral Blood Flow and Metabolism. 2006;26(6):857-63.
66. Lindvall O, Kokaia Z. Neurogenesis following Stroke Affecting the Adult Brain. Cold Spring Harbor Perspectives in Biology. 2015;7(11):a019034.
67. Minger SL, Ekonomou A, Carta EM, Chinoy A, Perry RH, Ballard CG. Endogenous neurogenesis in the human brain following cerebral infarction. Regenerative medicine. 2007;2(1):69-74.
68. Sanai N, Nguyen T, Ihrie RA, Mirzadeh Z, Tsai H-H, Wong M, et al. Corridors of migrating neurons in the human brain and their decline during infancy. Nature. 2011;478(7369):382-6.
69. Quinones-Hinojosa A, Sanai N, Soriano-Navarro M, Gonzalez-Perez O, Mirzadeh Z, Gil-Perotin S, et al. Cellular composition and cytoarchitecture of the adult human subventricular zone: a niche of neural stem cells. The Journal of comparative neurology. 2006;494(3):415-34.
70. Wu K-J, Yu S, Lee J-Y, Hoffer B, Wang Y. Improving Neurorepair in Stroke Brain Through Endogenous Neurogenesis-Enhancing Drugs. Cell transplantation. 2017;26(9):1596-600.
71. Huang L, Wong S, Snyder EY, Hamblin MH, Lee J-P. Human neural stem cells rapidly ameliorate symptomatic inflammation in early-stage ischemic-reperfusion cerebral injury. Stem cell research & therapy. 2014;5(6):129-.
72. Leong WK, Henshall TL, Arthur A, Kremer KL, Lewis MD, Helps SC, et al. Human adult dental pulp stem cells enhance poststroke functional recovery through non-neural replacement mechanisms. Stem cells translational medicine. 2012;1(3):177-87.
73. Arvidsson A, Collin T, Kirik D, Kokaia Z, Lindvall O. Neuronal replacement from endogenous precursors in the adult brain after stroke. Nature medicine. 2002;8(9):963-70.
74. Lundberg C, Martinez-Serrano A, Cattaneo E, McKay RD, Bjorklund A. Survival, integration, and differentiation of neural stem cell lines after transplantation to the adult rat striatum. Experimental neurology. 1997;145(2 Pt 1):342-60.
75. Fortin JM, Azari H, Zheng T, Darioosh RP, Schmoll ME, Vedam-Mai V, et al. Transplantation of Defined Populations of Differentiated Human Neural Stem Cell Progeny. Scientific reports. 2016;6:23579-.
76. Luo Y, Kuo C-C, Shen H, Chou J, Greig NH, Hoffer BJ, et al. Delayed treatment with a p53 inhibitor enhances recovery in stroke brain. Annals of neurology. 2009;65(5):520-30.
77. Schabitz WR, Steigleder T, Cooper-Kuhn CM, Schwab S, Sommer C, Schneider A, et al. Intravenous brain-derived neurotrophic factor enhances poststroke sensorimotor recovery and stimulates neurogenesis. Stroke. 2007;38(7):2165-72.
78. Zhang L, Hu X, Luo J, Li L, Chen X, Huang R, et al. Physical exercise improves functional recovery through mitigation of autophagy, attenuation of apoptosis and enhancement of neurogenesis after MCAO in rats. BMC neuroscience. 2013;14:46-.
79. Ma CL, Ma XT, Wang JJ, Liu H, Chen YF, Yang Y. Physical exercise induces hippocampal neurogenesis and prevents cognitive decline. Behavioural brain research. 2017;317:332-9.
80. Vizoso FJ, Eiro N, Cid S, Schneider J, Perez-Fernandez R. Mesenchymal Stem Cell Secretome: Toward Cell-Free Therapeutic Strategies in Regenerative Medicine. International journal of molecular sciences. 2017;18(9):1852.
81. Gervois P, Wolfs E, Ratajczak J, Dillen Y, Vangansewinkel T, Hilkens P, et al. Stem Cell-Based Therapies for Ischemic Stroke: Preclinical Results and the Potential of Imaging-Assisted Evaluation of

Donor Cell Fate and Mechanisms of Brain Regeneration. Medicinal research reviews. 2016;36(6):1080-126.
82. Gao F, Chiu SM, Motan DA, Zhang Z, Chen L, Ji HL, et al. Mesenchymal stem cells and immunomodulation: current status and future prospects. Cell death & disease. 2016;7:e2062.
83. Zhang Y, Qiu B, Wang J, Yao Y, Wang C, Liu J. Effects of BDNF-Transfected BMSCs on Neural Functional Recovery and Synaptophysin Expression in Rats with Cerebral Infarction. Molecular neurobiology. 2017;54(5):3813-24.
84. Bach LA. Current ideas on the biology of IGFBP-6: More than an IGF-II inhibitor? Growth hormone & IGF research : official journal of the Growth Hormone Research Society and the International IGF Research Society. 2016;30-31:81-6.
85. Zhang X, Zhou Y, Li H, Wang R, Yang D, Li B, et al. Intravenous administration of DPSCs and BDNF improves neurological performance in rats with focal cerebral ischemia. International journal of molecular medicine. 2018;41(6):3185-94.
86. Ikeda N, Nonoguchi N, Zhao MZ, Watanabe T, Kajimoto Y, Furutama D, et al. Bone marrow stromal cells that enhanced fibroblast growth factor-2 secretion by herpes simplex virus vector improve neurological outcome after transient focal cerebral ischemia in rats. Stroke. 2005;36(12):2725-30.
87. Golpanian S, Wolf A, Hatzistergos KE, Hare JM. Rebuilding the Damaged Heart: Mesenchymal Stem Cells, Cell-Based Therapy, and Engineered Heart Tissue. Physiological reviews. 2016;96(3):1127-68.
88. Martin-Montanez E, Pavia J, Santin LJ, Boraldi F, Estivill-Torrus G, Aguirre JA, et al. Involvement of IGF-II receptors in the antioxidant and neuroprotective effects of IGF-II on adult cortical neuronal cultures. Biochimica et biophysica acta. 2014;1842(7):1041-51.
89. Lin TN, He YY, Wu G, Khan M, Hsu CY. Effect of brain edema on infarct volume in a focal cerebral ischemia model in rats. Stroke. 1993;24(1):117-21.
90. Ziegler AN, Feng Q, Chidambaram S, Testai JM, Kumari E, Rothbard DE, et al. Insulin-like Growth Factor II: An Essential Adult Stem Cell Niche Constituent in Brain and Intestine. Stem cell reports. 2019;12(4):816-30.
91. Ziegler AN, Levison SW, Wood TL. Insulin and IGF receptor signalling in neural-stem-cell homeostasis. Nat Rev Endocrinol. 2015;11(3):161-70.
92. Ziegler AN, Chidambaram S, Forbes BE, Wood TL, Levison SW. Insulin-like growth factor-II (IGF-II) and IGF-II analogs with enhanced insulin receptor-a binding affinity promote neural stem cell expansion. J Biol Chem. 2014;289(8):4626-33.
93. Bach LA, Headey SJ, Norton RS. IGF-binding proteins – the pieces are falling into place. Trends in Endocrinology & Metabolism. 2005;16(5):228-34.
94. Bach LA. Recent insights into the actions of IGFBP-6. J Cell Commun Signal. 2015;9(2):189-200.
95. Fu P, Thompson JA, Bach LA. Promotion of cancer cell migration: an insulin-like growth factor (IGF)-independent action of IGF-binding protein-6. J Biol Chem. 2007;282(31):22298-306.
96. Francis GL, Aplin SE, Milner SJ, McNeil KA, Ballard FJ, Wallace JC. Insulin-like growth factor (IGF)-II binding to IGF-binding proteins and IGF receptors is modified by deletion of the N-terminal hexapeptide or substitution of arginine for glutamate-6 in IGF-II. Biochem J. 1993;293 (Pt 3)(Pt 3):713-9.
97. Lehtinen MK, Zappaterra MW, Chen X, Yang YJ, Hill AD, Lun M, et al. The cerebrospinal fluid provides a proliferative niche for neural progenitor cells. Neuron. 2011;69(5):893-905.
98. Marqués-Torrejón MÁ, Porlan E, Banito A, Gómez-Ibarlucea E, Lopez-Contreras AJ, Fernández-Capetillo O, et al. Cyclin-dependent kinase inhibitor p21 controls adult neural stem cell expansion by regulating Sox2 gene expression. Cell stem cell. 2013;12(1):88-100.
99. Fanarraga ML, Avila J, Zabala JC. Expression of unphosphorylated class III β-tubulin isotype in neuroepithelial cells demonstrates neuroblast commitment and differentiation. European Journal of Neuroscience. 1999;11(2):516-27.
100. Bid HK, Zhan J, Phelps DA, Kurmasheva RT, Houghton PJ. Potent inhibition of angiogenesis by the IGF-1 receptor-targeting antibody SCH717454 is reversed by IGF-2. Mol Cancer Ther. 2012;11(3):649-59.
101. Herr F, Baal N, Reisinger K, Lorenz A, McKinnon T, Preissner KT, et al. hCG in the Regulation of Placental Angiogenesis. Results of an In Vitro Study. Placenta. 2007;28:S85-S93.
102. Apolonia L, Waddington SN, Fernandes C, Ward NJ, Bouma G, Blundell MP, et al. Stable gene transfer to muscle using non-integrating lentiviral vectors. Molecular therapy : the journal of the American Society of Gene Therapy. 2007;15(11):1947-54.
103. Godecke N, Hauser H, Wirth D. Stable Expression by Lentiviral Transduction of Cells. Methods in molecular biology (Clifton, NJ). 2018;1850:43-55.
104. Hamaguchi I, Woods NB, Panagopoulos I, Andersson E, Mikkola H, Fahlman C, et al. Lentivirus vector gene expression during ES cell-derived hematopoietic development in vitro. Journal of virology. 2000;74(22):10778-84.
105. Dull T, Zufferey R, Kelly M, Mandel RJ, Nguyen M, Trono D, et al. A third-generation lentivirus vector with a conditional packaging system. Journal of virology. 1998;72(11):8463-71.
106. Robinson CR, Sligar SG. Molecular Recognition Mediated by Bound Water: A Mechanism for Star Activity of the Restriction Endonuclease EcoRI. Journal of Molecular Biology. 1993;234(2):302-6.
107. Fuchs ROY, Blakesley R. 2 - Guide to the Use of Type II Restriction Endonucleases. In: Wu R, Grossman L, Moldave K, editors. Recombinant DNA Methodology. San Diego: Academic Press; 1989. p. 25-60.
108. Fluri F, Schuhmann MK, Kleinschnitz C. Animal models of ischemic stroke and their application in clinical research. Drug Des Devel Ther. 2015;9:3445-54.
109. Caballero-Garrido E, Pena-Philippides JC, Galochkina Z, Erhardt E, Roitbak T. Characterization of long-term gait deficits in mouse dMCAO, using the CatWalk system. Behavioural brain research. 2017;331:282-96.

110. Doyle KP, Buckwalter MS. A mouse model of permanent focal ischemia: distal middle cerebral artery occlusion. Methods in molecular biology (Clifton, NJ). 2014;1135:103-10.
111. Morancho A, García-Bonilla L, Barceló V, Giralt D, Campos-Martorell M, Garcia S, et al. A new method for focal transient cerebral ischaemia by distal compression of the middle cerebral artery. Neuropathology and Applied Neurobiology. 2012;38(6):617-27.
112. Witty M. THE PROCESS FOR 2, 3, 5-TRIPHENYLTETRAZOLIUM CHLORIDE SYNTHESIS, AN INTELLECTUAL PROPERTY SEIZED IMMEDIATELY AFTER WORLD WAR II. Bull Hist Chem. 2012;37(2):91.
113. Kent TA, Mandava P. Embracing Biological and Methodological Variance in a New Approach to Pre-Clinical Stroke Testing. Translational stroke research. 2016;7(4):274-83.
114. Li C, Zhang YX, Yang C, Hao F, Chen SS, Hao Q, et al. Intraventricular administration of endoneuraminidase-N facilitates ectopic migration of subventricular zone-derived neural progenitor cells into 6-OHDA lesioned striatum of mice. Experimental neurology. 2016;277:139-49.
115. Duan W, Zhang YP, Hou Z, Huang C, Zhu H, Zhang CQ, et al. Novel Insights into NeuN: from Neuronal Marker to Splicing Regulator. Molecular neurobiology. 2016;53(3):1637-47.
116. Nito C, Sowa K, Nakajima M, Sakamoto Y, Suda S, Nishiyama Y, et al. Transplantation of human dental pulp stem cells ameliorates brain damage following acute cerebral ischemia. Biomedicine & pharmacotherapy = Biomedecine & pharmacotherapie. 2018;108:1005-14.
117. Guler HP, Zapf J, Schmid C, Froesch ER. Insulin-like growth factors I and II in healthy man. Estimations of half-lives and production rates. Acta endocrinologica. 1989;121(6):753-8.
118. Casimiro I, Chinnasamy P, Sibinga NES. Genetic inactivation of the allograft inflammatory factor-1 locus. Genesis. 2013;51(10):734-40.
119. Alexander M, Forster C, Sugimoto K, Clark HB, Vogel S, Ross ME, et al. Interferon regulatory factor-1 immunoreactivity in neurons and inflammatory cells following ischemic stroke in rodents and humans. Acta neuropathologica. 2003;105(5):420-4.
120. Daigneault M, Preston JA, Marriott HM, Whyte MKB, Dockrell DH. The identification of markers of macrophage differentiation in PMA-stimulated THP-1 cells and monocyte-derived macrophages. PloS one. 2010;5(1):e8668-e.
121. Li F, Yang M, Wang L, Williamson I, Tian F, Qin M, et al. Autofluorescence contributes to false-positive intracellular Foxp3 staining in macrophages: a lesson learned from flow cytometry. Journal of immunological methods. 2012;386(1-2):101-7.
122. Michalski D, Pitsch R, Pillai DR, Mages B, Aleithe S, Grosche J, et al. Delayed histochemical alterations within the neurovascular unit due to transient focal cerebral ischemia and experimental treatment with neurotrophic factors. PloS one. 2017;12(4):e0174996-e.
123. Huang L, Wu Z-B, Zhuge Q, Zheng W, Shao B, Wang B, et al. Glial scar formation occurs in the human brain after ischemic stroke. Int J Med Sci. 2014;11(4):344-8.